Validation Report - HIRS FDR Release 1

DOI: 10.15770/EUM_SEC_CLM_0026

Doc.No. : EUM/OPS/DOC/20/1179880
Issue : v4 e-signed
Date : 11 July 2022
WBS/DBS :

EUMETSAT
Eumetsat-Allee 1, D-64295 Darmstadt, Germany
Tel: +49 6151 807-7
Fax: +49 6151 807 555
http://www.eumetsat.int

Document Change Record

Version	***Version Date** (as on profile)*	***DCR* No.** if applicable*	***Description of Changes***
v1	8 June 2020		First draft version
v2	18 December 2020		Version ready for internal review
v3	26 April 2022		Version ready for DRR
v4	11 July 2022		Final version for release

DCR = Document Change Request

Table of Contents

Table of Figures

Table of Tables

1 INTRODUCTION

1.1 Purpose and Scope

This document details the validation results for the first release of the Fundamental Data Record (FDR) of High Resolution Infrared Radiation Sounder (HIRS) on-board operational NOAA and Metop satellites, hereinafter referred to as HIRS FDR Release 1. The data record covers more than 40 years from 29 October 1978 to 31 December 2020. The validation is performed by time series analyses and by comparison to simulated observations using ERA5 reanalysis profiles as input for the radiative transfer calculations.

1.2 Structure of this Document

Section 1 Purpose and scope of this validation report
Section 2 Background information
Section 3 Validation Strategy
Section 4 Validation Results
Section 5 Summary and Conclusions
Section 6 References

1.3 Acronyms

Acronym	Meaning
ATBD	Algorithm Theoretical Baseline Document
ECMWF	European Centre for Medium-Range Weather Forecasts
ERA-CLIM	European Re-Analysis of global Climate observations
EUMETSAT	European Organisation for the Exploitation of Meteorological Satellites
FDR	Fundamental Data Record
HIRS	High resolution Infrared Radiation Sounder
IR	Infra-Red
NeDT	Noise Equivalent Differential Temperature
NWP	Numerical Weather Prediction
PUG	Product User Guide
RTM	Radiative Transfer Model
SRF	Spectral Response Function
WMO	World Meteorological Organisation
WV	Water Vapour

1.4 Definitions

The following definitions are used throughout the document.

Products types:

- **Fundamental Data Record** (FDR): from single-sensor series, a FDR consists of a consistently processed time series of sensor observations calibrated to physical units, located in time and space, with suitable corrections applied, and possibly with uncertainty quantification[1].
    - Even FDRs covering a short period can prove essential, e.g., (a) to fill in gaps in the global observing system, (b) to ensure a consistent representation of variability in reanalysis or ECV products, (c) to provide an anchor to the assimilation in the case of variables/regions that are not observed by other sensors.
    - After initial/operational processing has been carried out a first time (possibly years or decades ago), producing a FDR is the first step towards the construction of a FCDR.

- **Fundamental Climate Data Record** (FCDR): from single-sensor or multiple-sensor series, a FCDR consists of a consistently processed time series of uncertainty-quantified sensor observations calibrated to physical units, located in time and space, and of sufficient length and quality to be directly useful for climate science or applications due to inclusion of reversible corrections obtained by homogenisation or harmonisation.
    - A FCDR is derived from one (or several) FDR(s).

[1] The Joint CEOS-CGMS Working Group on Climate issued this definition in 2020 but a written reference does not exist.

- A FCDR enables to produce a CDR of higher maturity (for the sake of climate applications) than a FDR.
- For assimilation into reanalysis, a FCDR may be left out in preference to a FDR, if there is the perception that the FCDR may contain corrections that are believed to be largely scene-dependent and better determined by an assimilation system.

2 BACKGROUND

In this chapter, background information is provided on the HIRS instrument, on the data that have been reprocessed and on the algorithms that have been used for the reprocessing. In order to improve the readability of the document, the reprocessing procedure is briefly summarized.

2.1 HIRS instruments

HIRS instruments are infrared sounding radiometers measuring radiation emitted or reflected by the Earth surface and its atmosphere in 20 spectral channels. Three generations of HIRS instruments are considered in this report: HIRS/2, HIRS/3, and HIRS/4.

HIRS/2 instruments were part of the TIROS Operational Vertical Sounder (TOVS; TIROS stands for Television Infrared Observation Satellites) suite. They were on-board TIROS-N and NOAA-6 to NOAA-14 (NOAA-13 failed to operate shortly after launch).

HIRS/3 instruments are enhanced version of the HIRS/2 instrument, operated on-board of NOAA-15 to NOAA-17. HIRS/3 is part of the ATOVS (Advanced TOVS) suite.

HIRS/4 instruments are the latest version and are operated on-board NOAA-18, NOAA-19, Metop-A, and Metop-B. The details of the different HIRS instruments is shown in Table 1 and Table 2.

Table 1 gives an overview of the main characteristics of the HIRS/2, HIRS/3, and HIRS/4 instruments. The optical field of view has been reduced for HIRS/4, which provides a higher pixel resolution. However, the sampling interval remains the same, which results in not observed areas between two pixels.

Table 1: Summary of the instrument characteristics of the HIRS instrument versions 2 to 4. Swath widths were calculated based on a satellite height of 830 km and assuming spherical earth of radius 6371km.

Characteristic	*HIRS/2*	*HIRS/3*	*HIRS/4*
Optical Field of View	*1.25 degrees*	*1.3 degrees (LW)* *1.4 degrees (SW)*	*0.69 degrees*
Earth Scan Angle	*±49.5 degrees from nadir*	*±49.5 degrees from nadir*	*±49.5 degrees from nadir*
Pixels/scan	*56*	*56*	*56*
Sampling interval	*1.8 degrees*	*1.8 degrees*	*1.8 degrees*
Scan rate	*6.4 seconds*	*6.4 seconds*	*6.4 seconds*
Earth Swath	*2232 km*	*2240 km*	*2204 km*
IFOV size	*17.4 km at nadir*	*20.3 km (1.4 degrees IFOV) at nadir for LW* *18.9 km (1.3 degrees IFOV) at nadir for SW*	*10 km at nadir*

Table 2 provides an overview on the central wavelengths of the HIRS channels. It should be mentioned here, that channel 12 (sensitive to upper-tropospheric water vapour) changes from HIRS/2 (6.73 µm) to HIRS/3 and HIRS/4 (6.52 µm), and that channel 10 (sensitive to lower-tropospheric water vapour) changes from HIRS/2 (8.21 µm) to HIRS/3 and HIRS/4 (12.47 µm).

Table 2: Summary of the central wavelength (in µm) for each spectral channel of the different HIRS instrument versions HIRS/2, HIRS/3, and HIRS/4.

Channel	*HIRS/2*	*HIRS/3*	*HIRS/4*
1	*14.97*	*14.96*	*14.96*
2	*14.71*	*14.71*	*14.70*
3	*14.48*	*14.49*	*14.49*
4	*14.19*	*14.23*	*14.23*
5	*13.94*	*13.97*	*13.97*
6	*13.65*	*13.64*	*13.64*
7	*13.36*	*13.35*	*13.35*
8	*11.10*	*11.11*	*11.11*
9	*9.71*	*9.71*	*9.71*
10	*8.21*	*12.47*	*12.47*
11	*7.31*	*7.33*	*7.33*
12	*6.73*	*6.52*	*6.52*
13	*4.57*	*4.57*	*4.57*
14	*4.53*	*4.53*	*4.53*
15	*4.47*	*4.47*	*4.47*
16	*4.41*	*4.45*	*4.45*
17	*4.24*	*4.13*	*4.13*
18	*3.98*	*3.98*	*3.98*
19	*3.77*	*3.76*	*3.76*
20	*0.69*	*0.69*	*0.69*

Based on [RD 5], note:

1. The exact channel definitions changed slightly between successive HIRS instruments.
2. There are two exceptions to Table 2: NOAA-11 and NOAA-14, in spite of branded as HIRS/2, feature similar characteristics as HIRS/3 regarding channels 10 and 17.

The reprocessing takes such information into account by applying for each channel the central wavelength that is specific to each satellite.

Table 3 shows the pre-launch specifications for the Noise Equivalent Differential Temperature (NEDT) at 280K for all instruments and channels (except channel 20 which is the a visible channel). These values are converted from the noise equivalent delta radiance, which are provided in the NOAA user guides (RD 4 and RD 5).

Table 3: *NEDT specifications for the 19 longwave channels of all HIRS instruments. These numbers are taken from RD 4 and RD 5. The noise equivalent delta radiances are converted to temperatures at 280K.*

	1	**2**	**3**	**4**	**5**	**6**	**7**	**8**	**9**	**10**	**11**	**12**	**13**	**14**	**15**	**16**	**17**	**18**	**19**
TIROSN	2	0.44	0.33	0.2	0.14	0.16	0.13	0.1	0.12	0.22	0.29	0.39	0.09	0.05	0.07	0.08	0.05	0.09	0.08
NOAA-06	2	0.44	0.33	0.2	0.14	0.16	0.13	0.1	0.12	0.22	0.29	0.39	0.09	0.05	0.07	0.08	0.05	0.09	0.08
NOAA-07	2	0.44	0.33	0.2	0.14	0.16	0.13	0.1	0.12	0.22	0.29	0.39	0.09	0.05	0.07	0.08	0.05	0.09	0.08
NOAA-08	2	0.44	0.33	0.2	0.14	0.16	0.13	0.1	0.12	0.22	0.29	0.39	0.09	0.05	0.07	0.08	0.05	0.09	0.08
NOAA-09	2	0.44	0.33	0.2	0.14	0.16	0.13	0.1	0.12	0.22	0.29	0.39	0.09	0.05	0.07	0.08	0.05	0.09	0.08
NOAA-10	2	0.44	0.33	0.2	0.14	0.16	0.13	0.1	0.12	0.22	0.29	0.39	0.09	0.05	0.07	0.08	0.05	0.09	0.08
NOAA-11	2	0.44	0.33	0.2	0.14	0.16	0.13	0.1	0.12	0.1	0.29	0.39	0.09	0.05	0.07	0.08	0.07	0.09	0.08
NOAA-12	2	0.44	0.33	0.2	0.14	0.16	0.13	0.1	0.12	0.22	0.29	0.39	0.09	0.05	0.07	0.08	0.05	0.09	0.08
NOAA-14	2	0.44	0.33	0.2	0.14	0.16	0.13	0.1	0.12	0.1	0.29	0.39	0.09	0.05	0.07	0.08	0.07	0.09	0.08
NOAA-15	2	0.44	0.33	0.2	0.14	0.16	0.13	0.07	0.12	0.1	0.29	0.44	0.09	0.05	0.07	0.07	0.07	0.09	0.08
NOAA-16	2	0.44	0.33	0.2	0.14	0.16	0.13	0.07	0.12	0.1	0.29	0.44	0.09	0.05	0.07	0.07	0.07	0.09	0.08
NOAA-17	2	0.44	0.33	0.2	0.14	0.16	0.13	0.07	0.12	0.1	0.29	0.44	0.09	0.05	0.07	0.07	0.07	0.09	0.08
NOAA-18	2	0.44	0.33	0.2	0.14	0.16	0.13	0.07	0.12	0.1	0.29	0.44	0.09	0.05	0.07	0.07	0.07	0.09	0.08
NOAA-19	2	0.44	0.33	0.2	0.14	0.16	0.13	0.07	0.12	0.1	0.29	0.44	0.09	0.05	0.07	0.07	0.07	0.09	0.08
METOP-A	2	0.44	0.33	0.2	0.14	0.16	0.13	0.07	0.12	0.1	0.29	0.44	0.09	0.05	0.07	0.07	0.07	0.09	0.08
METOP-B	2	0.44	0.33	0.2	0.14	0.16	0.13	0.07	0.12	0.1	0.29	0.44	0.09	0.05	0.07	0.07	0.07	0.09	0.08

2.2 HIRS calibration

The measurement principle of HIRS is discussed in detail in RD 4 (HIRS/2) and RD 5 (HIRS/3 and 4). The calibration of the HIRS infrared channels makes use of the warm blackbody and cold space views. This provides a two-point calibration yielding a calibration slope and intercept for each channel, which are used to convert instrument counts into radiance. Possible effects from a non-linear behaviour of the detector are not considered in the calibration, as they have been found insignificant during the pre-launch measurements.

In general, the so-called HIRS superswath, consisting of 40 scan lines in total, is considered for the calibration. The superswath starts with a calibration cycle that consists of a space view followed by a warm blackbody view (56 samples each), and then 38 Earth-view scan lines with 56 samples per scan line.

HIRS/2 data have an extra calibration scanline (so only 37 Earth view scanlines), observing an internal cold calibration target. Because it was found to be unstable over time, this internal cold calibration target has never been used for calibration.

Similar to the HIRS instruments, the calibration algorithms went through an evolution as well that resulted in four different versions. These algorithms mostly vary in how the calibration measurements in the superswaths are used as well as in how and if the instrument self-emission has been considered.

The ATBD [RD 1] provides information on algorithms used for generating the FDR from the HIRS/2, HIRS/3, and HIRS/4 instruments. A modified version of the version 4 (v4) calibration algorithm embedded in the ATOVS and AVHRR Pre-processing Package (AAPP) software provided by the NWP-SAF [RD 6] was used for the processing. This version enables to transfer the most recent operational calibration (v4; RD 11) algorithm to the HIRS/2 and HIRS/3 instruments. The AAPP HIRS calibration v4 algorithm was only applicable for the HIRS/3/4 data. This is one of the major improvements made to the HIRS/2 data in this FDR.

The main changes to the previous algorithms are:

- More than one calibration cycle is used to compute the calibration slope and offset, which reduces strong variations in the calibration coefficients between two or within a superswath;
- The instrument self-emission is considered and a model for computing its impact is implemented;
- The noise equivalent Differential temperature (NEDT), as a measure of the instrument noise, is computed and provided for every pixel and channel for all HIRS instruments, derived using both cold and warm calibration view measurements. This feature was introduced in AAPP v7.1 in November 2015, but a reprocessing of all HIRS data with this or later versions of AAPP has not been done till the realisation of this data record;
- The data quality control has been updated and applied throughout the FDR identically.

The impact of these changes is evaluated in this validation report.

2.3 Data coverage

The temporal coverage of the the HIRS FDR Release 1 is given in Table **4**.

Table 4: Temporal coverage of the HIRS FDR. The start and end years may not contain full coverage and there may be gaps in between which is reflected in the number of years.

Satellite	Instrument	Reprocessed Years	# of years
TIROS-N	HIRS/2	1978 - 1980	3
NOAA-06	HIRS/2	1979 - 1983	5
NOAA-07	HIRS/2	1981 – 1985	5
NOAA-08	HIRS/2	1983 – 1984	2
NOAA-09	HIRS/2	1985 - 1988	4
NOAA-10	HIRS/2	1986 - 1991	6
NOAA-11	HIRS/2	1988 - 1998	10
NOAA-12	HIRS/2	1981 - 1998	8
NOAA-14	HIRS/2	1995 - 2006	12
NOAA-15	HIRS/3	1999 - 2020	14
NOAA-16	HIRS/3	2001 - 2014	14
NOAA-17	HIRS/3	2002 - 2013	12
NOAA-18	HIRS/4	2005 - 2020	16
NOAA-19	HIRS/4	2009 - 2020	12
Metop-A	HIRS/4	2006 - 2020	15
Metop-B	HIRS/4	2013 - 2020	8
TOTAL		**1978 - 2020**	**143**

3 VALIDATION STRATEGY

This section summarises the validation strategy and introduces the data used to evaluate the HIRS FDR Release 1. The data quality of the FDR is evaluated by three separate approaches:

- Time series analysis of FDR brightness temperatures and comparison to operationally calibrated data (original) brightness temperatures;
- Comparison to simulated observations;
- Recalibration impact analysis.

3.1 Validation datasets

This section summarises the data sets that are used for the validation of the HIRS FDR Release 1.

3.1.1 Original data (AAPP/ATOVIN processing)

In this report, the 'original data' is meant by the NOAA CLASS Level 1b data processed by the AAPP software module ATOVIN. ATOVIN applies the operational calibration coefficients to the measurement counts to obtain radiances and then to brightness temperatures producing the output files in HDF format. Note that the operational calibration of the HIRS instruments evolved over time as discussed in RD 11.

The analysis of the 'original data' indicate two findings: (1) for some periods, especially in the first years of the HIRS/3 operation, the NEDT is not available (NOAA-15/16/17 until mid of 2005); and (2) the quality flag "chanqual" is flagging a large amount of data, especially of the later instruments, as "marginal calibration view counts".

3.1.2 Simulated Brightness Temperatures

In this study, the simulations of HIRS measurements are performed using the radiative transfer model RTTOV version 13.0 (RD 7), which is developed within the EUMETSAT NWP-SAF. The atmospheric background is described by reanalysis profiles from ERA5 (RD 9). The CAMEL surface emissivity atlas (version 2; RD 12) describes the surface emissivity.

The radiance simulator software version 3 (RD 8) provided by the EUMETSAT NWP-SAF is used to perform the RTTOV simulations. This simulator uses, as inputs, the reanalysis fields of a specific time and an observation file, which contains the geolocation and time of each HIRS measurement to be simulated. Internally, the radiance simulator interpolates the model fields spatially to the nearest observation point. Only those reanalysis profiles which are within ±1 hour of pixel measurements are used for simulation.

As the HIRS instrument measures close to the CO_2 absorption line at 15µm, the varying CO_2 concentrations in the atmosphere are considered as well. The CO_2 concentrations are taken from the NOAA CO_2 climatology (NOAA-ESRL Global Monitoring; Monthly Average Mauna Loa CO2), which provides monthly mean CO_2 amounts.

3.2 Validation methods

As mentioned above, three approaches are used to validate the HIRS FDR. For consistency, and unless specified otherwise, the following analysis considers only those measurements that pass all quality controls and cloud screening.

3.2.1 Time series analysis and comparison to original data

The HIRS FDR Release 1 is firstly assessed by analysing the time series of the brightness temperature. This analysis reveals the quality of the FDR in terms of temporal stability, shows inter-satellite biases, discontinuities, short term trends (natural or due to technical issues), single sensor stability, and peaks or short period jumps. For such a long time series as for HIRS (more than 4 decades), all these points affect the overall quality. Additionally, the warm target NEDT is shown as a time series with the specifications included as grey shaded area in the background. The time series per sensor show the mean brightness temperature or NEDT for all observations of one day that pass the quality control. The results are presented in section 4.1.

3.2.2 Comparison to simulated observations

Findings from this method must be interpreted bearing in mind their limitations, two in particular. First, HIRS data were assimilated into ERA5, which means the comparison is not independent, keeping in mind however that biases were removed by variational bias correction in the ERA5 reanalysis and the data were thinned before assimilation. Second, important assumptions are used in the radiative transfer, such as clear sky. This introduces a dependence of the results on the quality of the cloud screening as shown afterwards.

The clear-sky simulations are compared to clear-sky HIRS measurements. The results are shown as a function of time. Considering computational costs, the comparisons were limited to 4 synoptic hours per day[2] and to one profile in every grid of a 0.5 degree equal-area grid[3]. Statistics computed on a daily basis are shown after applying a 10-point moving average.

Several **quality controls (QC)** are applied:

QC1. This quality control consists in removing so-called “noisy episodes”. This is achieved by discarding data (a) for 160 scan lines (equivalent to 4 calibration cycles) before and after situations when the channel calibration quality flag (“chanqual”) is non-zero, and (b) for a given channel/satellite/day when the corresponding cold or warm NEDT average (for the channel/satellite/day) exceeds instrumental specifications (RD 5) by more than 10%. This 10% margin is a conservative measure to avoid discarding too many points in this report. It is noted that data users may wish to consider this example and/or experiment with other settings for their own application area. The impact of this step is shown in sections 4.2 and 4.3.

QC2. Only cloud free observations are used. The cloud detection method, applied in this study, is a modified version of the old HIRS cloud detection scheme of ECMWF (RD 10). The modified cloud detection scheme is based on two screening tests, which reject data if one of the tests indicate clouds. The first test sets the limits for the channel 8 first-guess departure (measurement – simulation) to -1K and +2K. The second test requires that the absolute first-guess departure of channel 8 must

[2] +/- 1 hour around 00, 06, 12, and 18 UTC; this reduces the number of daily profiles to simulate by a factor close to 3
[3] this further reduces the number of daily profiles to simulate by a factor close to 2

be lower than 3 times the expected standard deviation of the clear-sky first-guess departure in channel 8. This is set to 0.84K. This truncation of the distribution of differences for channel 8, to only retain small values, means the mean and standard deviation of the residual data bring no information. Consequently, channel 8 is omitted in the presentation of the results.

QC3. Further, daytime observations are excluded from the analysis for the shortwave sounding channels (shorter than 5 µm), as the solar radiation affects those observations and the simulation is not straightforward. In practice, this exclusion is realized by considering scenes where the solar zenith angle is larger than 100 degrees.

QC4. Finally, to restrict the comparison to conditions that can be simulated with a good quality, simulations that are known to of poor quality were excluded from the comparison. Conditions that result in poor quality simulations are:

- For the water vapor channels (10 to 12): locations over high terrain (elevation greater than 1500 m);
- For the surface channels (18 and 19): locations over land.

3.2.3 Recalibration impact analysis

The applied HIRS calibration algorithm (version 4) has two major changes compared to the calibration algorithm applied to HIRS/2 sensors (RD 11). First, the self-emission is improved by a revised method. Second, multiple calibration cycles are considered to compute the calibration coefficients. The latter aims to reduce the impact of a single calibration cycle on the calibration coefficients, which could result in artificial discontinuities from scanline to scanline. More details are provided in the ATBD (RD 1). The impact of these improvements is evaluated by looking at the bias between the HIRS FDR and the original brightness temperatures as a function of scanline in the superswath. In the original data of the HIRS/2 instruments, the calibration coefficients of a calibration cycle are valid for the first half of the superswath. Whereas, the calibration coefficients in the second half of the superswath are based on the following calibration cycle. This potentially introduces a discontinuity in the calibrated radiances in the middle of the superswath and leads to erroneous calibration values. As the calibration algorithm, which is applied in the HIRS FDR processing, uses several calibration cycles to calculate the calibration coefficients, it is expected that this discontinuity will not be present anymore. Consequently, it is expected that the absolute bias between the HIRS FDR and the original data increases towards the centre of a superswath, changes significantly there, and decreases again towards the end of a superswath (see section 4.3).

4 PRODUCT VALIDATION RESULTS

The following subsections presents the results of the HIRS FDR data quality evaluations, based on the three means introduced in section 3.

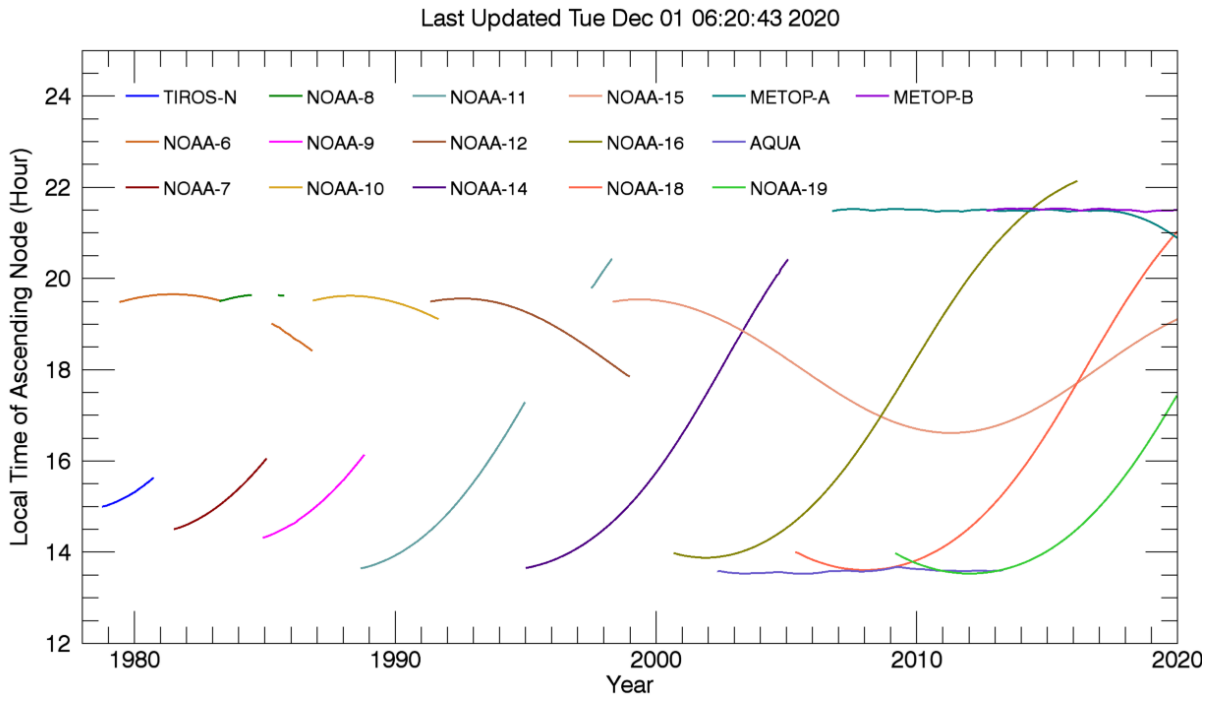

Figure 1: Equator crossing time of platforms that carry microwave sounders usable for upper air sounding. All except Aqua also include HIRS. [Source: http://www.remss.com/support/crossing-times/]

HIRS instruments have been operating on-board of polar orbiting satellites since the late 1970s. These satellites sometimes present significant drift. The orbital precession can be prevented (as done for recent satellites) but this requires sufficient fuel on the spacecraft. These drifts impact how the diurnal cycle is observed by sensors from low-Earth orbit (e.g., RD 14). This can lead to spurious changes in surface temperature or cloud patterns in the climate products, if this orbital drift is not accounted for. This can also cause apparent trends in the time series of single instruments, which depends on the channel, by aliasing the diurnal cycle into the climate change signal.

Figure 1 shows the orbits of all satellites, which carry the HIRS instrument (plus AQUA, which carries no HIRS). The figure shows the only times with microwave instruments and, thus, might not cover the same times at which HIRS instruments operated.

The measurements of HIRS instruments are affected by the thermal environment of the satellite/instrument, because the sensor self-emission contributes to the measurements themselves. The instrument temperature refers to the instrument base plate temperature and can be considered as an indicator of the temporal stability of the thermal environment of the satellite. Further, the instrument temperature is highly correlated to the secondary mirror temperature, which is used for estimating the sensor self-emission contribution in the calibration.

Figure 2 shows the instrument temperature of all data (mean temperature over one month of all data used in section 4.2). For the HIRS/2 instruments, the standard deviation is higher compared to HIRS/3 and 4 instruments.

HIRS on board of NOAA-15 revealed changes in the seasonal cycle between 2002 and 2008. This was probably related to the orbital drift of NOAA-15 from early morning to late afternoon, in which NOAA-15 passed the twilight zone. This resulted in a temperature difference of the spacecraft due to changing solar heating. A similar effect was observed for NOAA-12. HIRS on-board of NOAA-19 had a sudden increase in the instrument temperature in summer 2013. At the same time the HIRS quality dropped and the NEDT increased for several channels (e.g., see section 4.1.1).

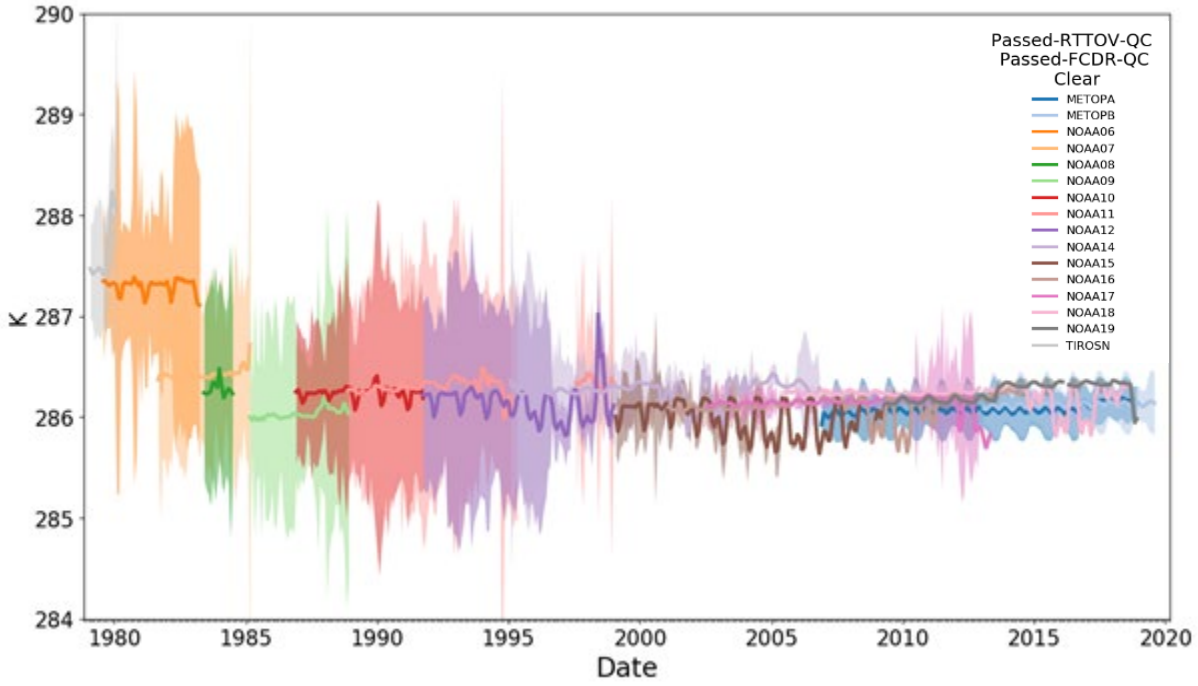

Figure 2: *Instrument temperature of all HIRS instruments. This quantity is not channel dependent.*

4.1 Time series analysis and comparison to original data

The next sections present the time series of the HIRS FDR for different spectral channels. The sections are grouped into temperature sounding channels, surface sensitive channels, ozone sensitive channels, water vapour sounding channels, and shortwave channels. The Figure presented in these sections includes two panels, showing the brightness temperature and the NEDT at the warm calibration target, as time series for a given channel. To be able to show features on small temperature scale, the value range on the y-axes is optimised for each channel and is neither for the temperature nor for the NEDT identical for all channels.

The software, used to process the FDR, provides a quality flag, which reports on the calibration quality (bit 1 and 2 in chanqual; see Appendix D in RD 2). The count measurements of each calibration scanlines are compared to the noise specifications of the HIRS instrument. If the calibration count variability exceeds the specifications, the calibration scanline is flagged. This quality flag was not available in this form in the operational NOAA CLASS data files. In the HIRS FDR this quality flag is only set for the calibration scanlines and not for the earth view

scan lines. One option could be to apply this quality flag to the surrounding 40 scanlines (one super swath). An alternative option, yielding similar results, is to use the warm target NEDT in the data file to filter scanlines with larger noise. The latter approach is much easier for a user to implement, because NEDT is available for every scanline, and, thus, is applied in the presentation of the results below. Further, the user can decide on the threshold of noise that is accepted for any downstream applications. For example, applications accumulating data, such as monthly means, can accept higher noise, than applications using single measurements, such as data assimilation applications. As a reference, Table 3 provides the NEDT specifications as published by NOAA.

Figure 3 to Figure 5 demonstrate the impact of this filtering on HIRS brightness temperatures of NOAA-18 on 01.01.2010 for the channels 4, 8, and 12. They show the decrease in available data using different NEDT quality thresholds. This day refers to a phase of NOAA-18 with increased noise, and for this reason one expects that many data shall be excluded by this filtering step. As one reduces the NEDT quality threshold, fewer data pass the filtering. On the other hand, this means that the data that successfully pass the filter are less noisy. We illustrate this here with two NEDT quality thresholds: "1*NEDT" means that only data with NEDT lower than the specification are shown, and "1.25*NEDT" means only data with NEDT lower than 1.25 times the specification are shown.

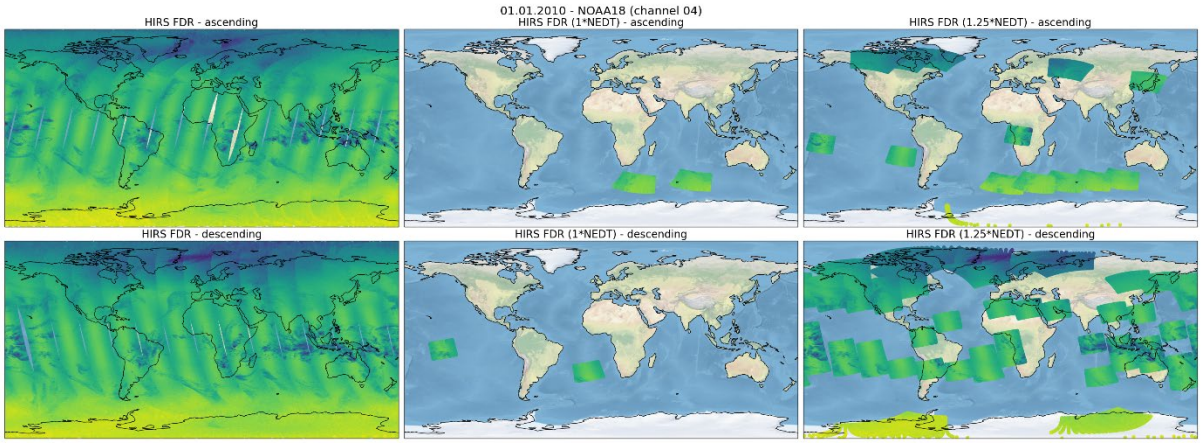

Figure 3: *Maps showing the brightness temperature of the HIRS FDR for channel 4 on NOAA-18 on 01.01.2010. From left to right: no NEDT filtering applied; all scanlines with NEDT > specifications removed; all scanlines with NEDT > 125% of the specification removed.*

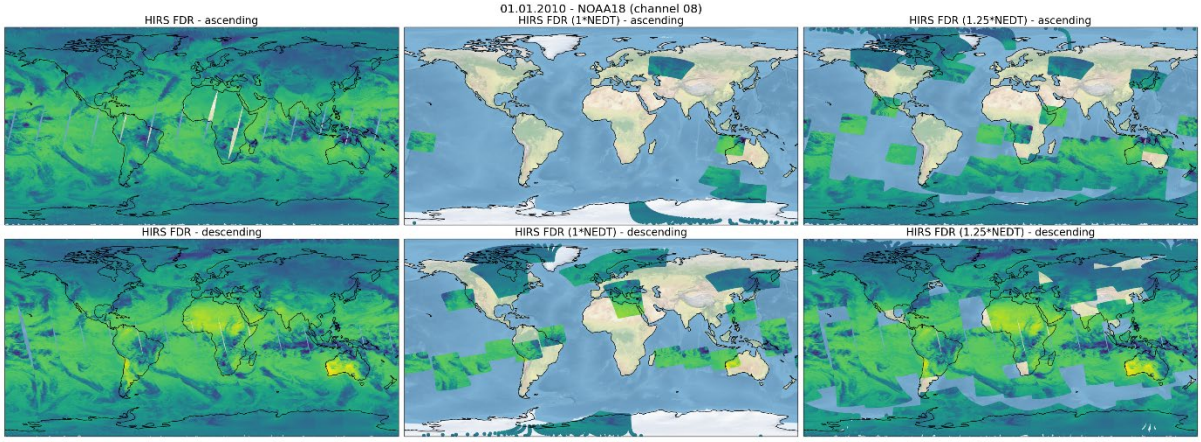

Figure 4: *Maps showing the brightness temperature of the HIRS FDR for channel 8 on NOAA-18 on 01.01.2010. From left to right: no NEDT filtering applied; all scanlines with NEDT > specifications removed; all scanlines with NEDT > 125% of the specification removed.*

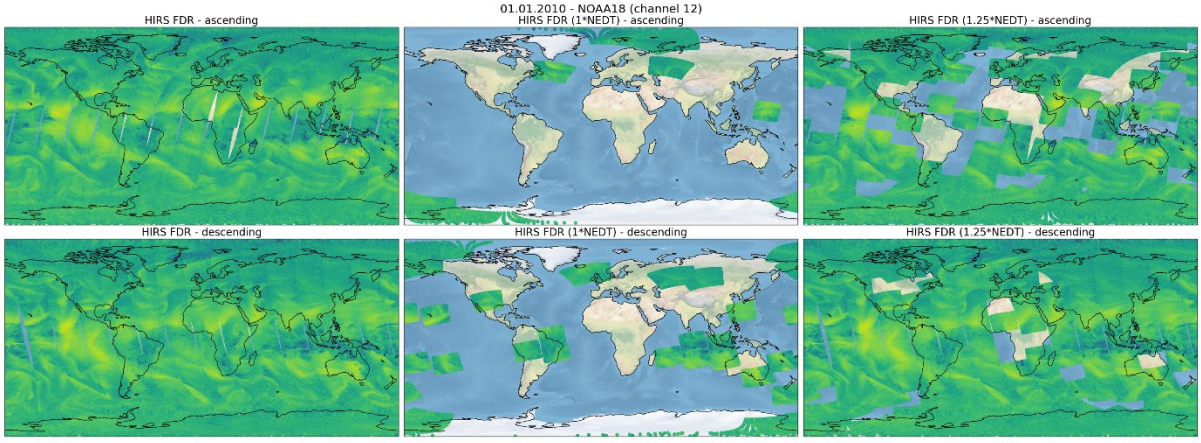

Figure 5: *Maps showing the brightness temperature of the HIRS FDR for channel 12 on NOAA-18 on 01.01.2010. From left to right: no NEDT filtering applied; all scanlines with NEDT > specifications removed; all scanlines with NEDT > 125% of the specification removed.*

If number of super swaths, passing the quality check (NEDT < 125% of specification), is low, the brightness temperature, averaged over one day, might not be comparable to other days. To account for this in the time series, shown below, only those daily means are included, for which at least 40% of the data passed the quality checks. This limitation has been chosen for presentation of the results in this report and does not mean that those rejected daily means include bad quality data. It must be mentioned, that the users should decide on usage of the data based on the application as written above.

4.1.1 Temperature sounding channels (channel 1 to 7)

Figure 6 to Figure 12 show the results for the longwave temperature sounding channels. For some channels, the sensor-to-sensor differences as well as the time series of single sensors is stable. For other channels (1, 4, and 5) the differences between sensors can exceed the amplitude of the annual cycle. Single sensors show mostly a high stability with almost no jumps and only a few peaks. Peaks can be caused by varying sample size for the statistics, i.e. is less valid data points are available for the daily means. One example of observations with large sensor noise in some channels is NOAA-12 in 1997 and 1998. During this period, the NEDT

values increased around 1K to 2K for most channels but up to 12K in channel 1. Consequently, these data are excluded from the brightness temperature time series. The source of these increased NEDT values is the filter wheel for the long wave channels, which is out-of-sync due to lubrication starvation. After 2017, HIRS on-board of Metop-A shows larger NEDT values. Also for NOAA-18, we found that the NEDT values peak several times, and for NOAA-19 the NEDT values jumps up in July 2013 and stays for most channels on a higher level afterwards. The NEDTs of NOAA-19 decrease slowly for most channels and are within the specifications from end of 2019. For NOAA-19, the remaining brightness temperature measurements show for several channels useful data and a mostly stable time series. Nevertheless, in the NEDT plot an increased noise could be identified, which makes the brightness temperatures less reliable in certain periods. For NOAA-18, the remaining brightness temperatures show for most channels large variability in the time series and these data should be used with caution.

Additionally, for several channels the inter-satellite difference can be large. This is mostly caused by spectral differences between the HIRS instruments or by changes between the instrument versions (e.g. HIRS/2 to HIRS/3). Section 4.2 analyses these spectral differences.

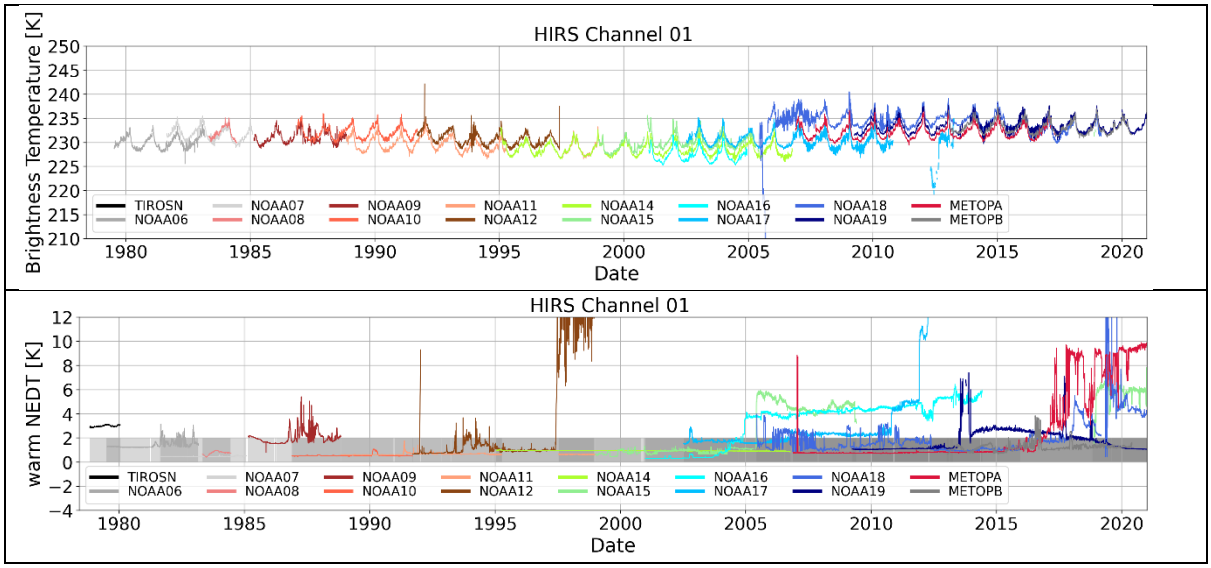

Figure 6: *Time series of channel 1 of the HIRS FDRs. Shown is the brightness temperatures (top) and the warm target NEDT (bottom).*

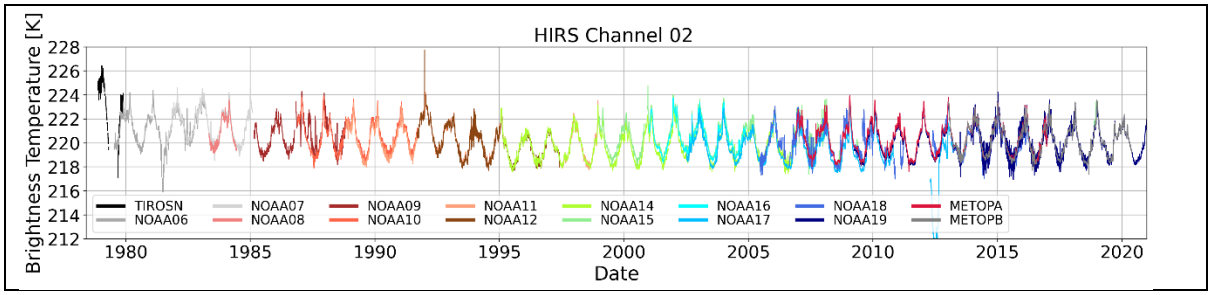

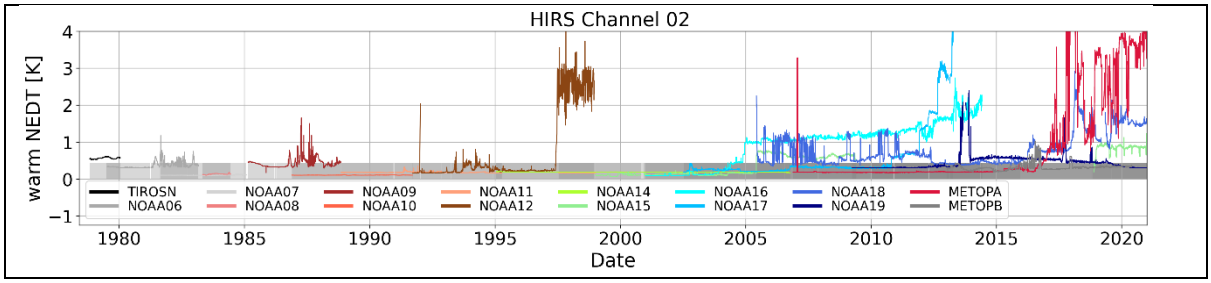

Figure 7: *same as Figure 1, but for channel 2.*

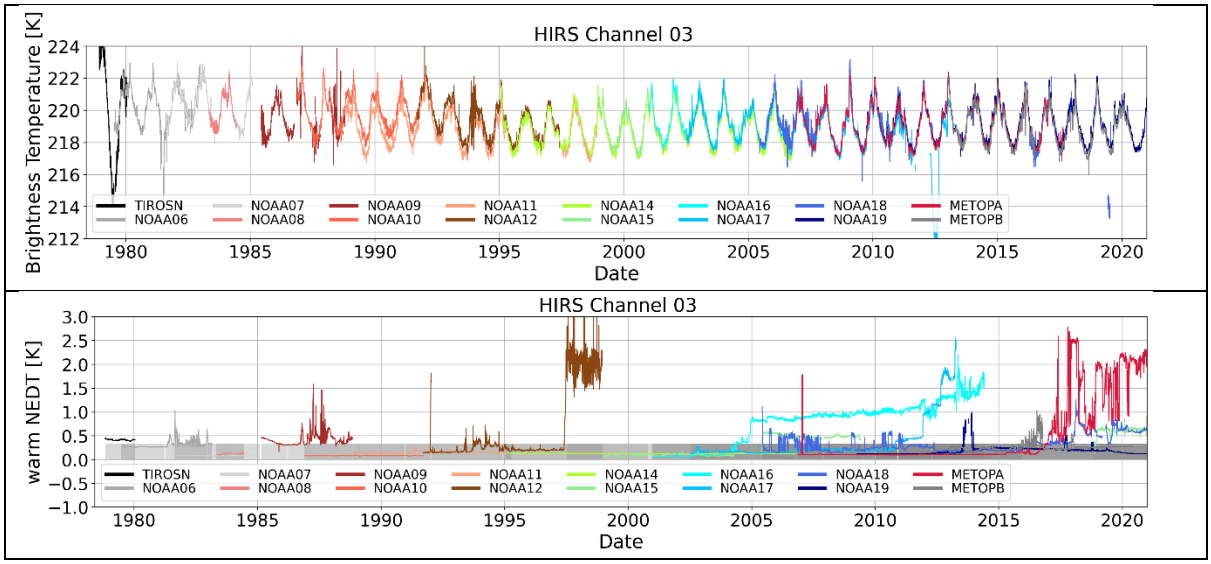

Figure 8: *same as Figure 1, but for channel 3.*

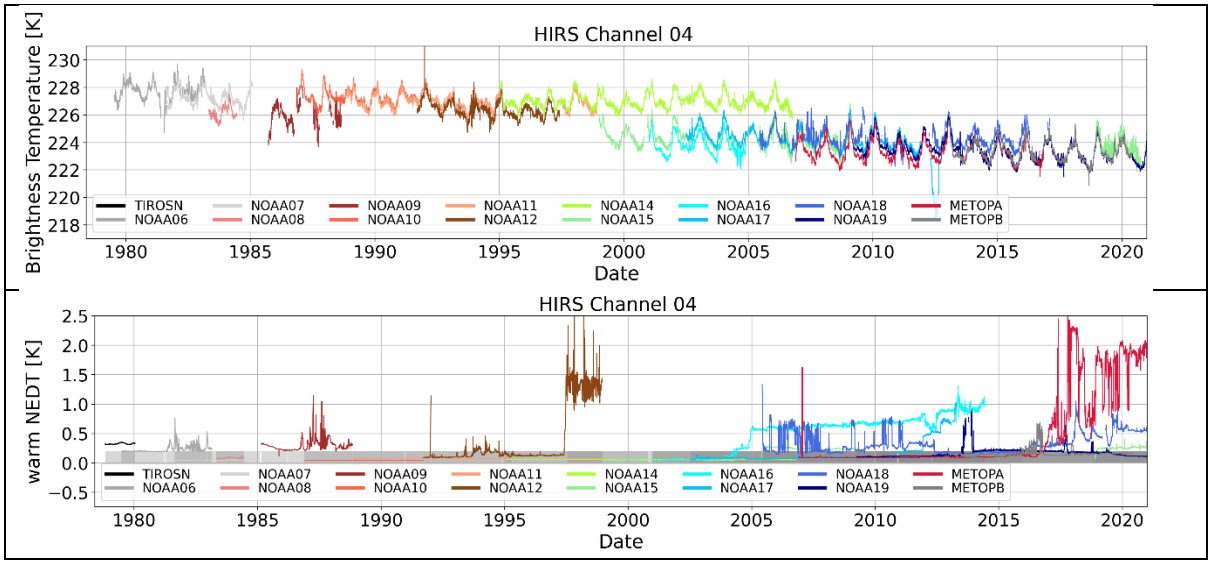

Figure 9: *same as Figure 1, but for channel 4.*

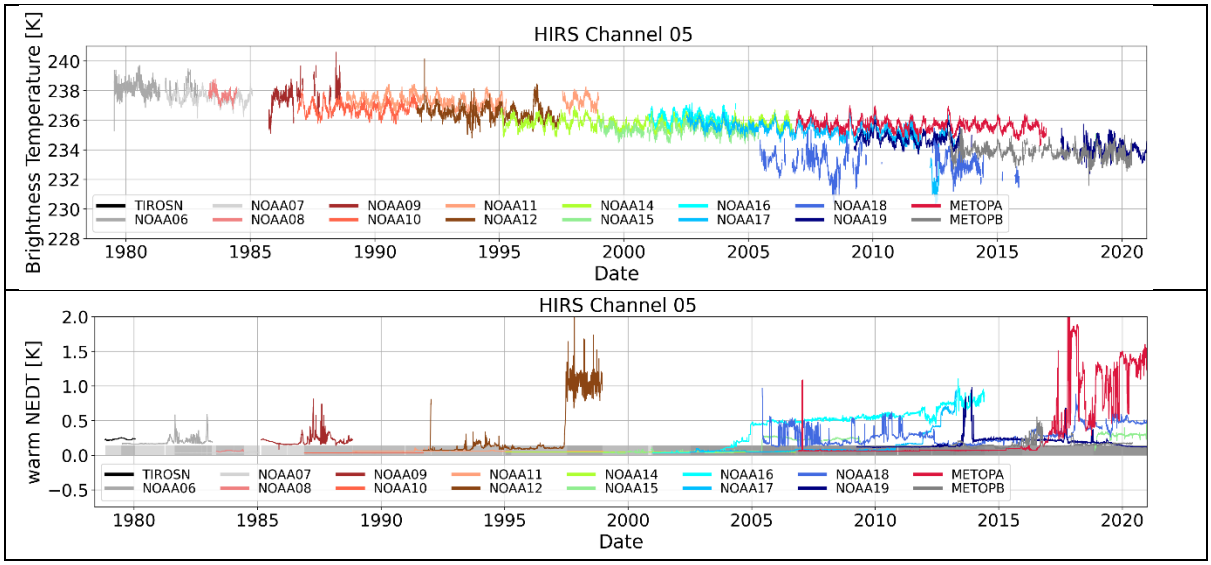

Figure 10: *same as Figure 1, but for channel 5.*

The time series for channel 4 shows a negative trend. The only exception is NOAA14 with no trend. This is also seen in the comparison against simulations (see section 4.2.1). As channel 4 is sensitive in the lower stratosphere and the upper troposphere, this trend is expected to be smaller compared to other temperature-sounding channels sensitive to mid or lower troposphere.

The temperature time series in channel 5 (Figure 10) shows a clear negative trend over the decades. Channel 5 is most sensitive in the troposphere between 400 and 600 hPa. In addition, the channels 6 and 7 show this trend, but much weaker and dominating after 2005. Channel 6 and 7 are sensitive to the mid and lower troposphere. The trend in channels 4 to 7 is likely related to the changing CO2 concentration in the troposphere and associated changes in the atmosphere [see discussions in RD 15].

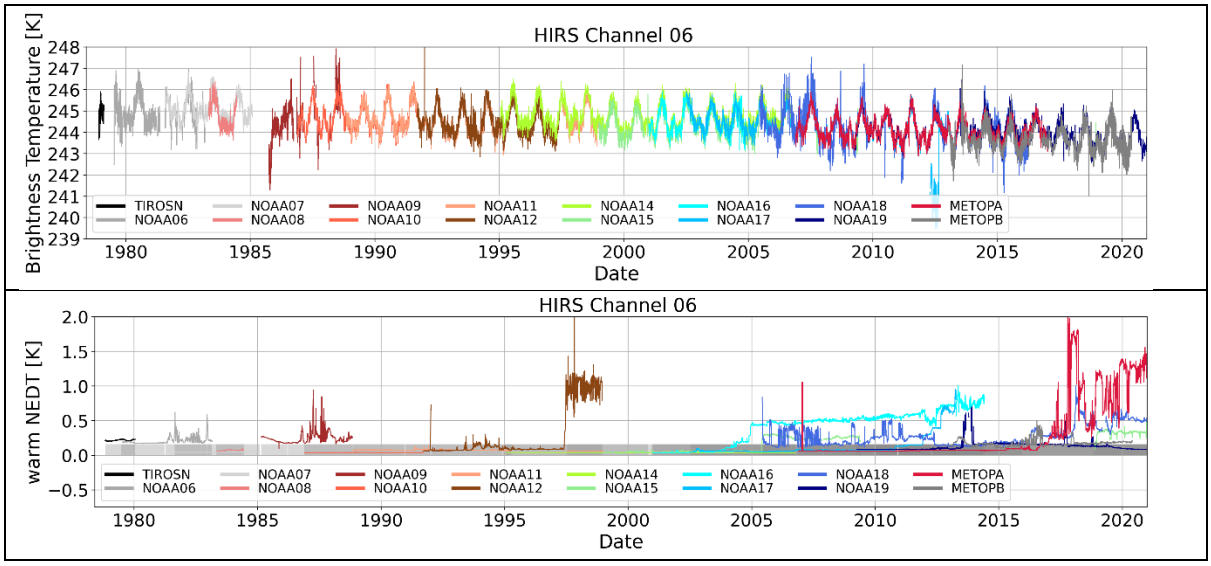

Figure 11: *same as Figure 1, but for channel 6.*

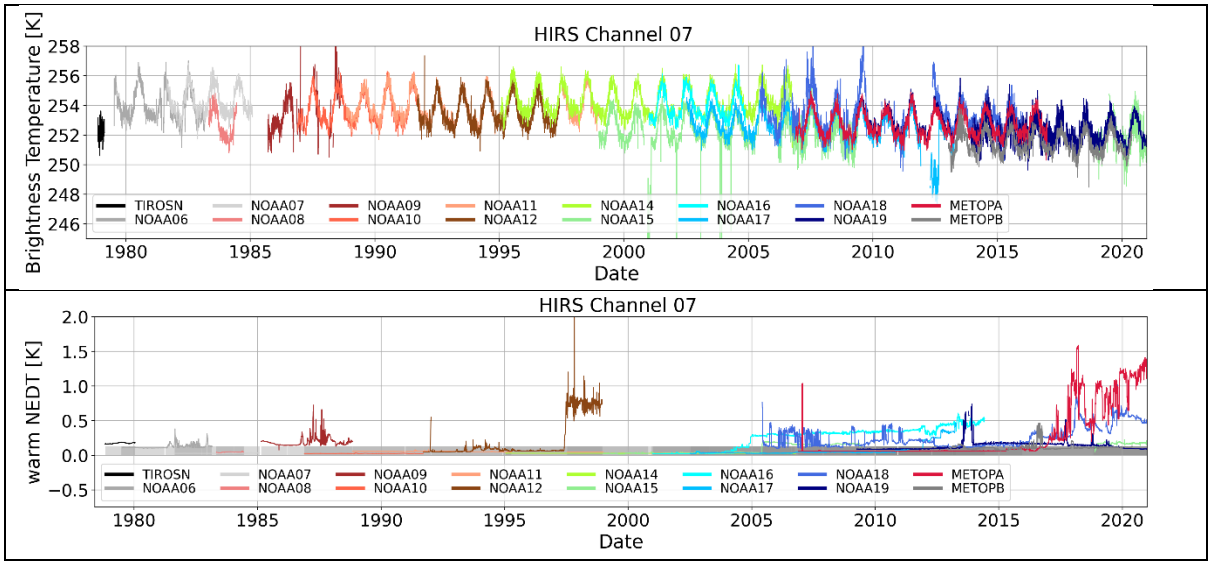

Figure 12: *same as Figure 1, but for channel 7.*

4.1.2 Surface sensitive channel (channel 8)

Figure 13 shows the HIRS time series for channel 8, which measures in the thermal window and is sensitive down to the surface in the cloud free conditions. This channel shows a very stable time series with a very constant annual cycle. The time series of the NEDTs show the above mentioned features for NOAA-12, -18, -19, and Metop-A for channel 8 as well.

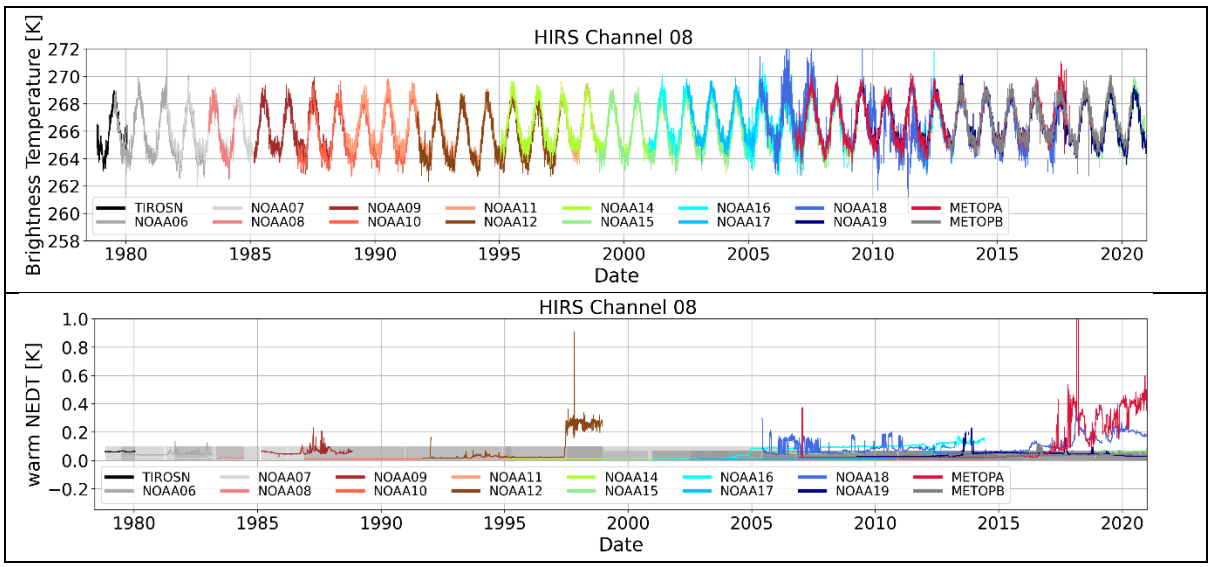

Figure 13: *same as Figure 1, but for channel 8.*

4.1.3 Ozone sensitive channel (channel 9)

Figure 14 shows the HIRS time series for channel 9, which is sensitive to the ozone content in atmosphere. Channel 9 has a similar performance as channel 8.

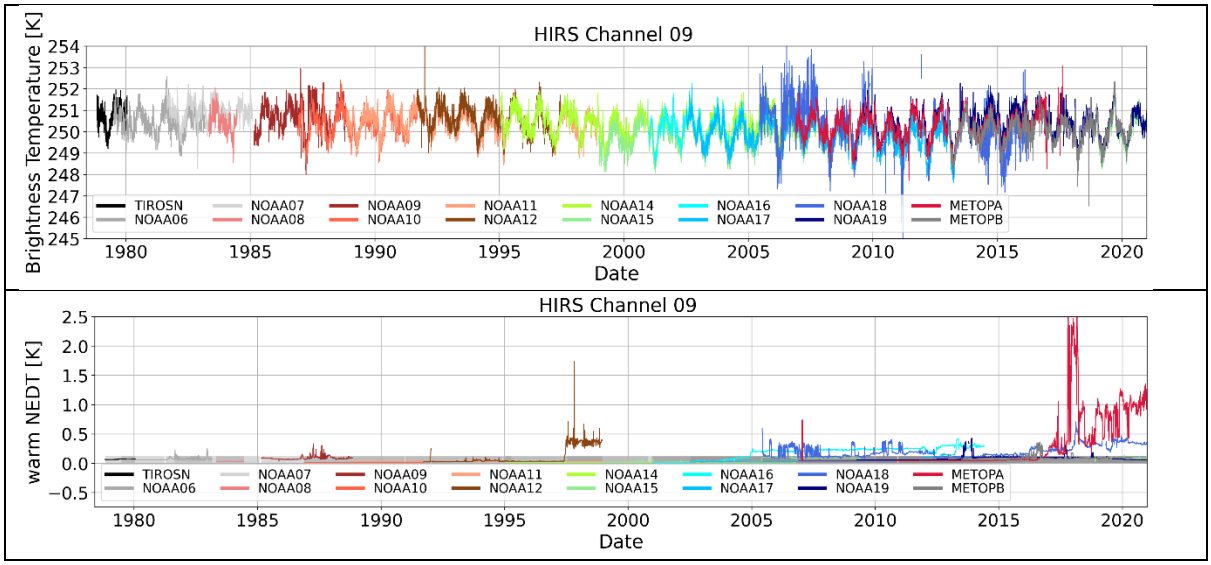

Figure 14: *same as Figure 1, but for channel 9.*

4.1.4 Water vapor sounding channels (channel 10 to 12)

Figure 15 to Figure 17 show the HIRS time series for the water vapour sounding channels, with channel 12 being most sensitive to the upper tropospheric humidity and channel 10 most sensitive to the lower troposphere. Channel 10 changed the central frequency from HIRS/2 (8.3µm) to HIRS/3 (12.5µm), which causes no clear offset as both observe the water vapour in the lower troposphere. Channel 12 was moved from 6.7µm to 6.5µm, which introduces a 6-8 K offset [RD 16].

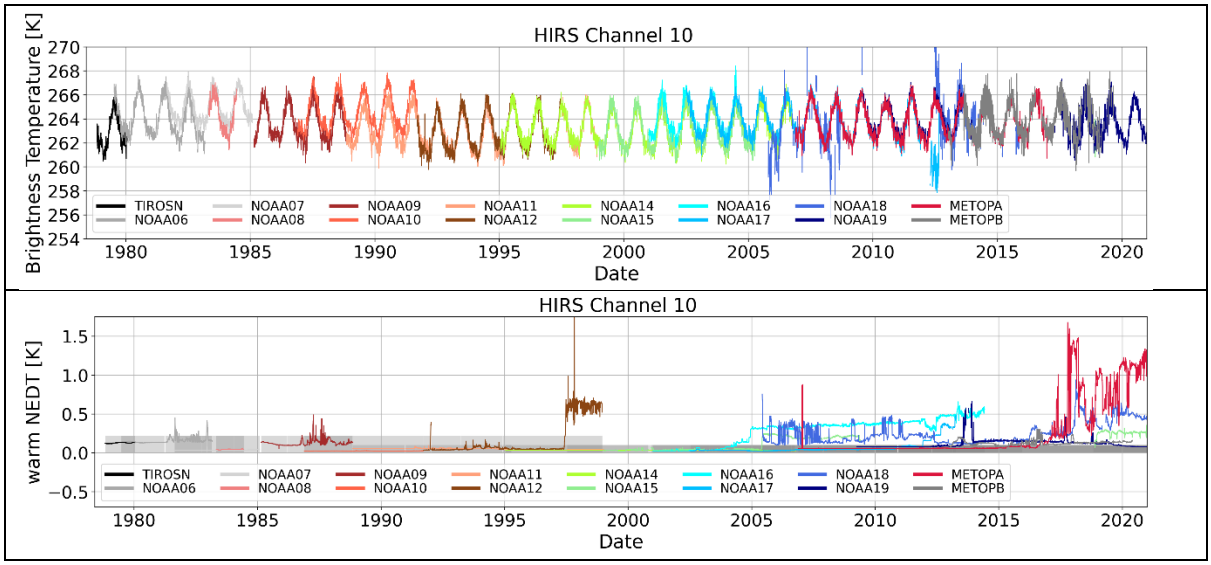

Figure 15: *same as Figure 1, but for channel 10.*

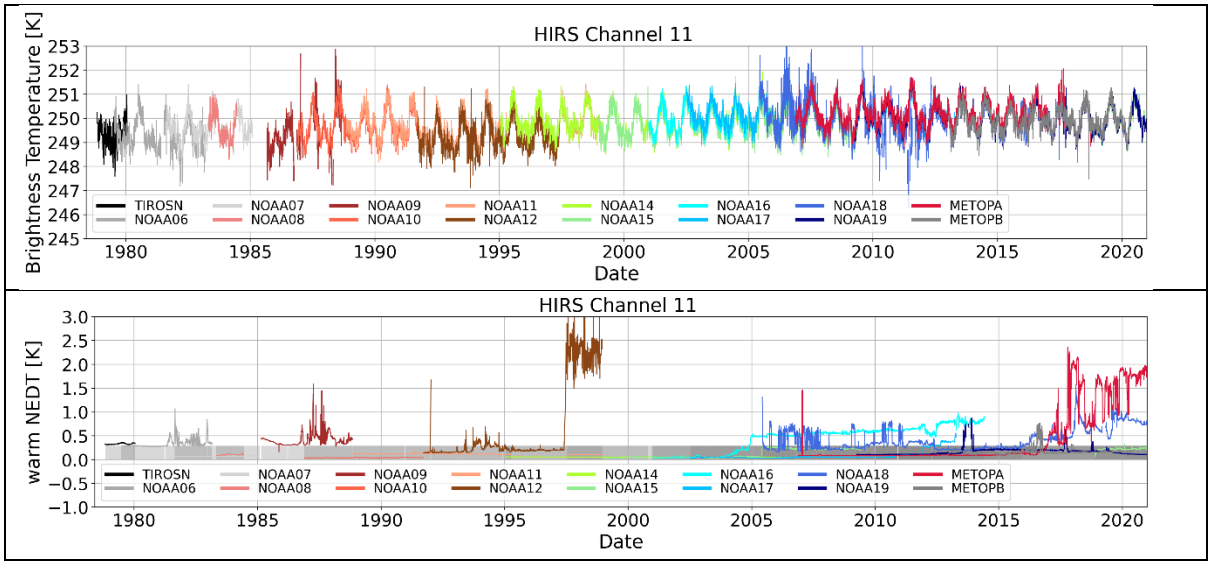

Figure 16: *same as Figure 1, but for channel 11.*

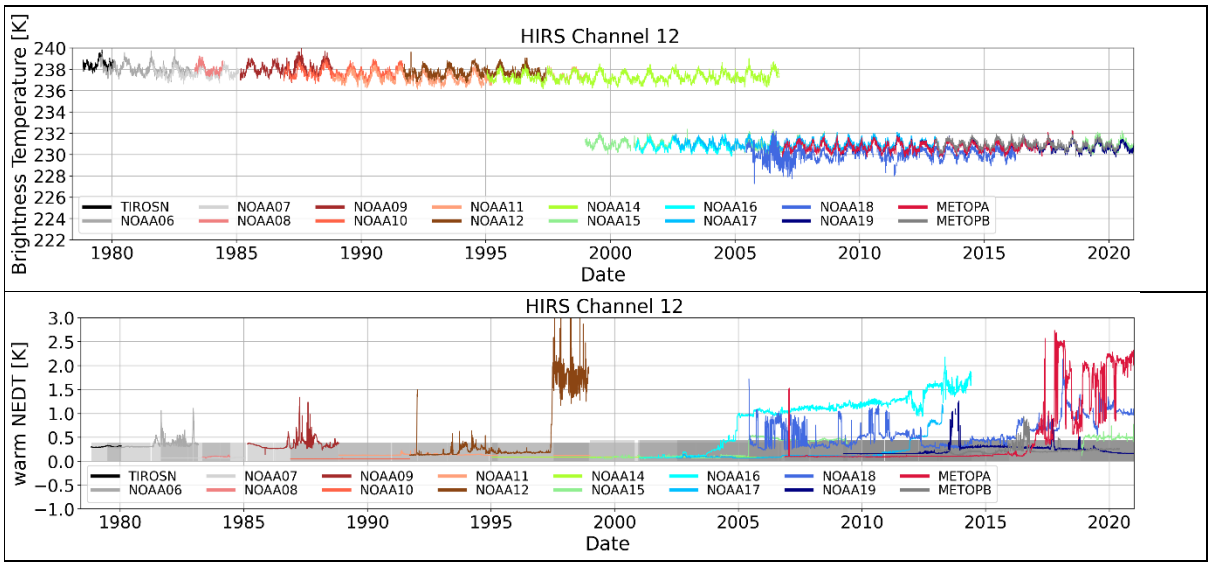

Figure 17: *same as Figure 1, but for channel 12.*

4.1.5 Shortwave (temperature sounding) channels (channel 13 – 19)

Figure 18 to Figure 24 show the HIRS time series for the shortwave temperature sounding channels 13 to 19. The shortwave channels show similar features as were found for the longwave channels. The largest features come from the inter-satellite difference. The shortwave temperature sounding channels have a narrower spectral response functions (SRF), than the longwave channels. Thus, small changes in the central wavenumber can cause larger differences in the measured brightness temperatures. Also the NEDTs are out of specifications for some periods, as mentioned above (late years of NOAA-12, -18, and Metop-A). The most obvious feature is channel 16 on-board NOAA-9, which is 20 K warmer than HIRS/2 and 10 K warmer than HIRS/3. As per [RD 18], the Channel 16 on NOAA-9 is defective.

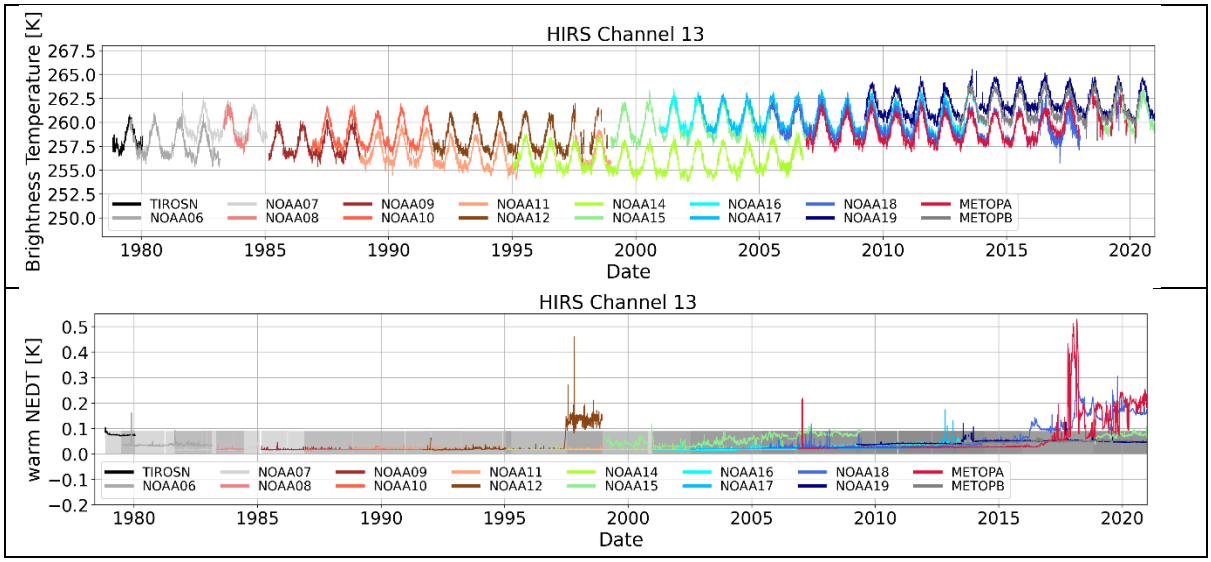

Figure 18: *same as Figure 1, but for channel 13.*

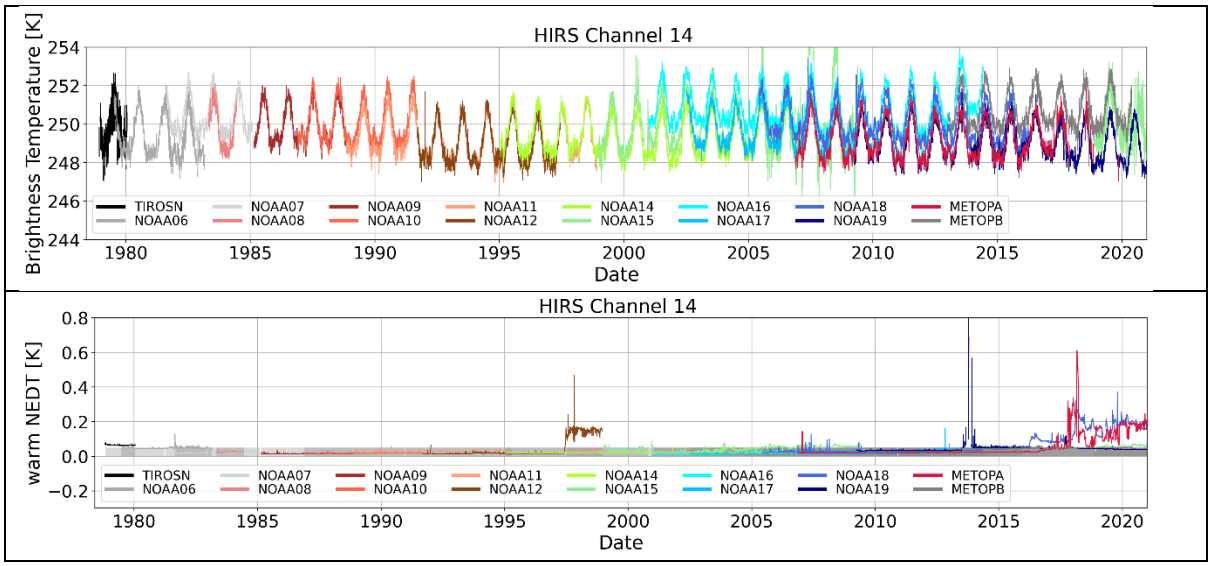

Figure 19: *same as Figure 1, but for channel 14:*

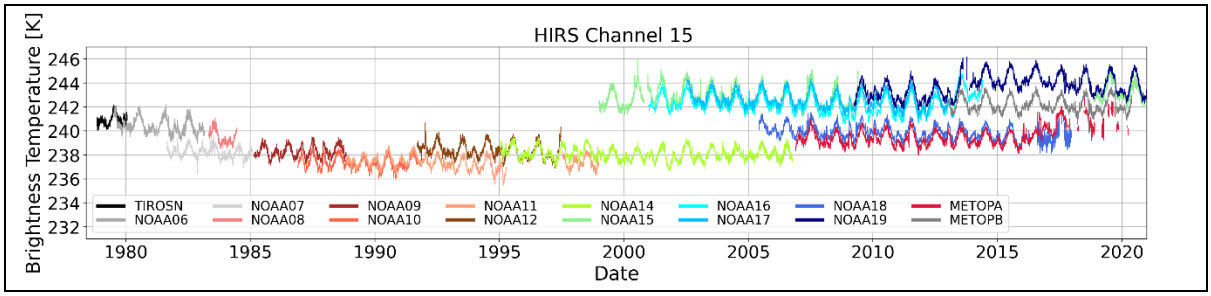

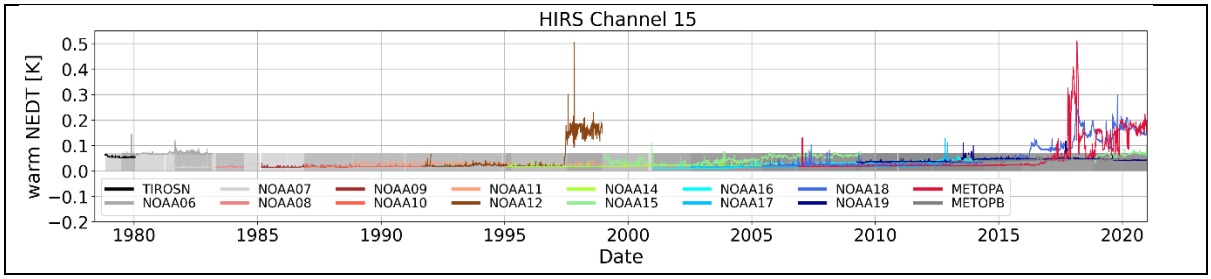

Figure 20: *same as Figure 1, but for channel 15.*

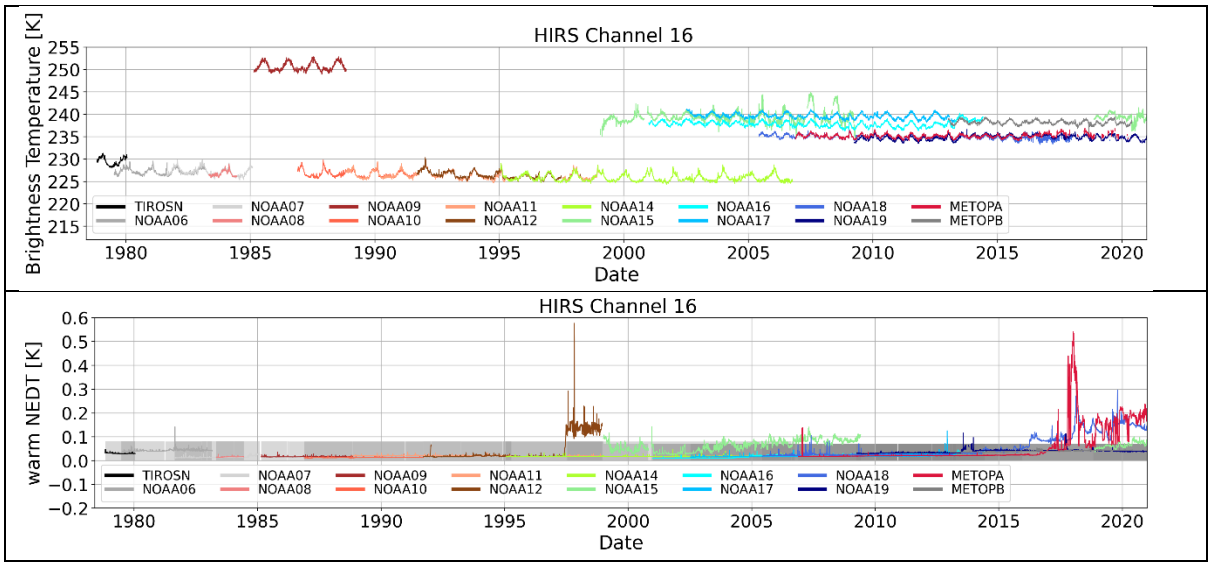

Figure 21: *same as Figure 1, but for channel 16.*

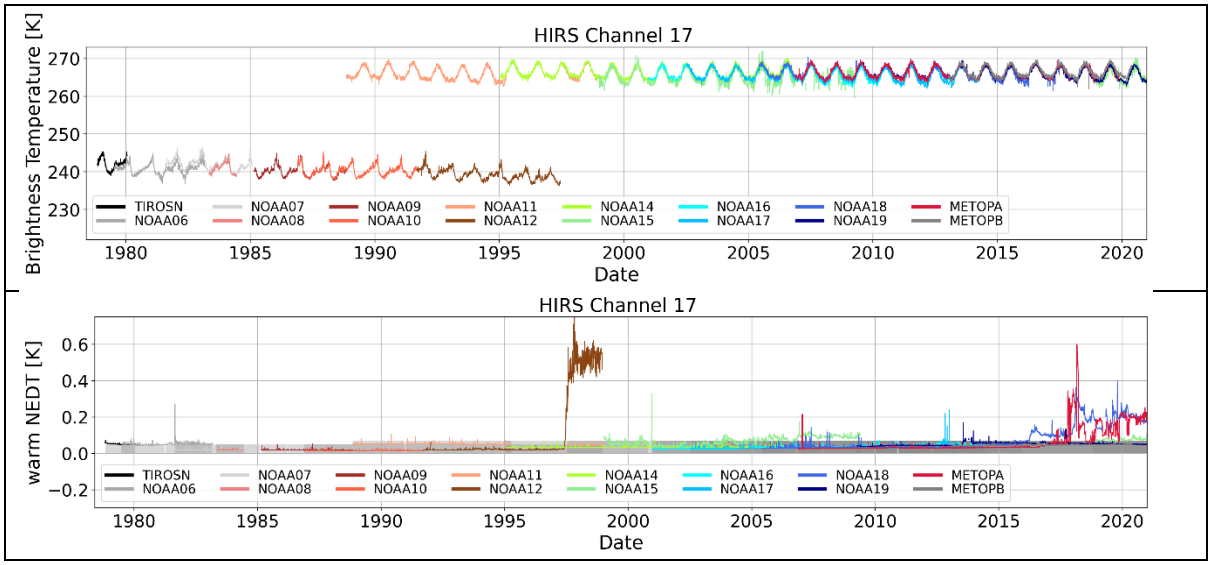

Figure 22: *same as Figure 1, but for channel 17.*

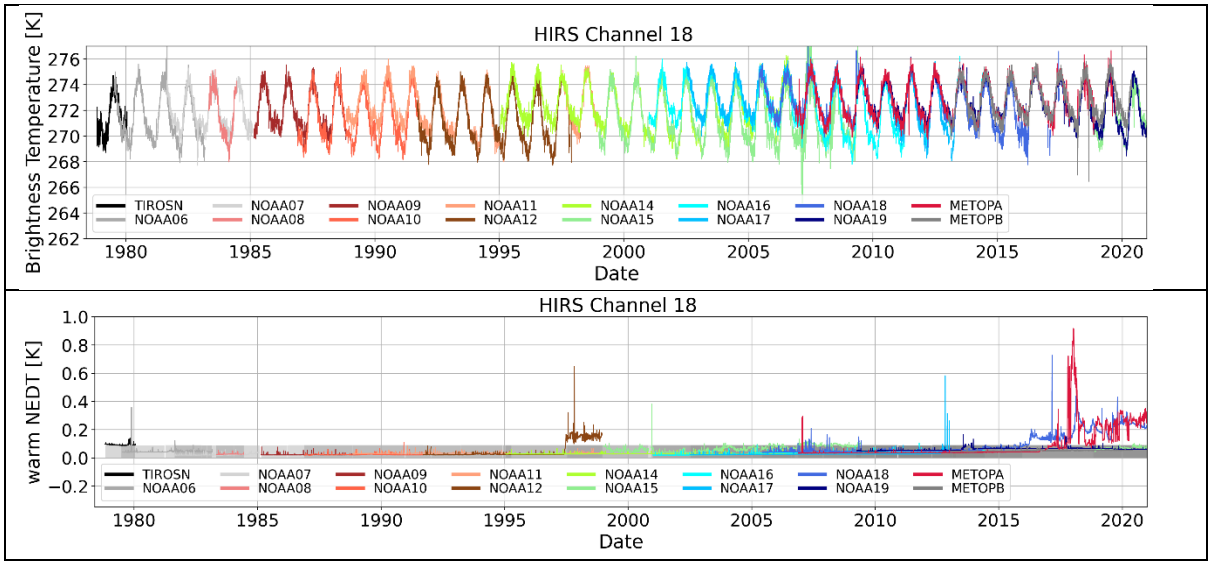

Figure 23: *same as Figure 1, but for channel 18.*

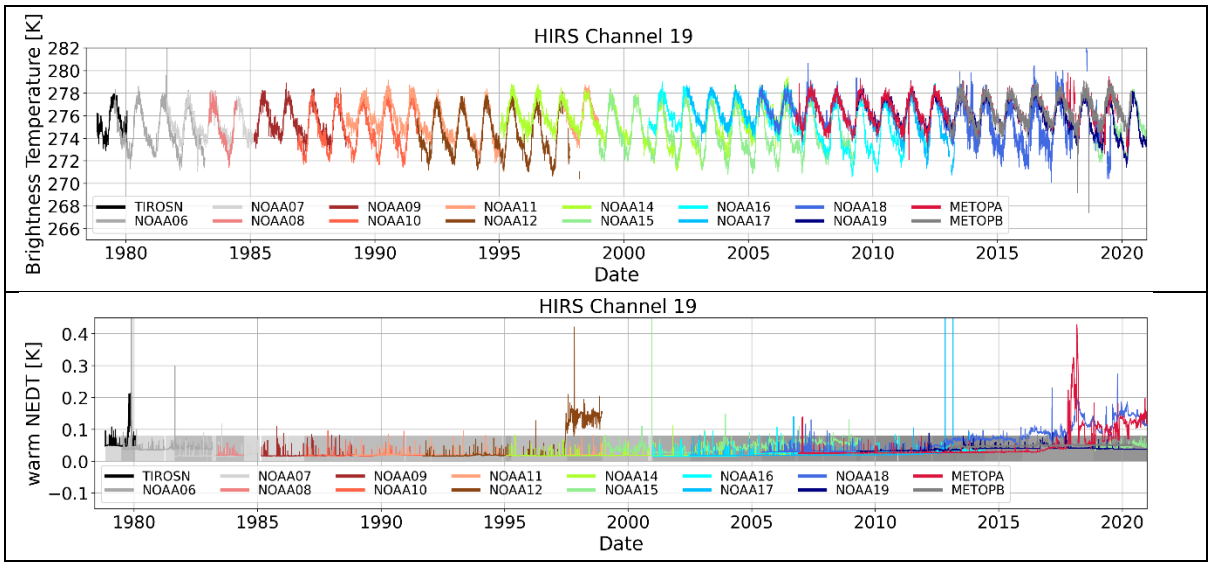

Figure 24: *same as Figure 1, but for channel 19.*

4.2 Comparison to simulated observations

This section focuses on the comparison of the HIRS FDR data against simulated observations. The simulations are performed as described in section 3.1.2 and section 3.2.2. Quality controls QC1 to QC4 are applied, unless otherwise specified.

In the following subsections, the bias to the simulated observations is analysed as a function of time. The channels are split into two groups: (a) longwave temperature sounding (channels 1 to 7) and water vapour sounding (channels 10 to 12), in section 4.2.1, and (b) surface-sensitive (channels 18 and 19), ozone (channel 9) and shortwave (channel 13 to 17), in section 4.2.2.

The channels are ordered by their sensitivity from top (sensitive to the lower stratosphere or upper troposphere) to bottom (most sensitive near the surface).

Each subsection starts with the time series of the number of observations per day, which passed the quality controls and cloud screening. Further, the biases (with standard error) are shown. In the end, the standard deviation is shown, as well as with mean NEDT (with standard error).

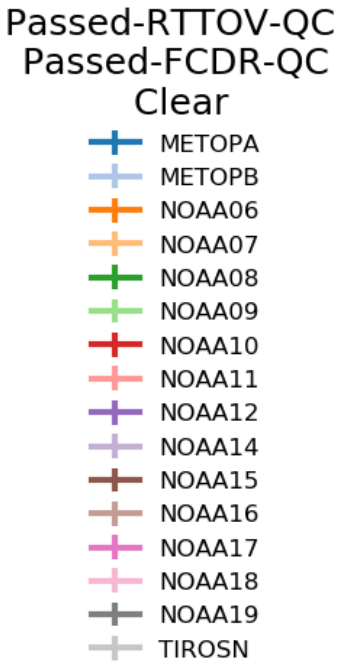

Figure 25: *legend for the comparisons to simulated observations.*

For all coming results in section 4.2, Figure 25 provides the legend. Note the error bars are only included in the mean plots (and not standard deviation plots); the bar indicates +/- one time the standard error of the mean.

4.2.1 Longwave temperature and water vapour sounding channels

The number of observations in the analysis (Figure 26) is very stable with time. The drop in data counts around 1991 is caused by the Mount Pinatubo eruption that year, with many profiles failing the cloud screening. This is due to volcanic aerosols observed by HIRS instruments on the one hand, but, on the other hand, aerosols not being included in the radiative transfer simulations. This indicates how the efficiency of cloud screening affects these comparisons.

The newer sensors (HIRS/3 and 4) show slightly more data than the older sensors (HIRS/2). This is most likely related to the third calibration scanline in HIRS/2 sensors, which is converted to an Earth view scanline in HIRS/3 and 4.

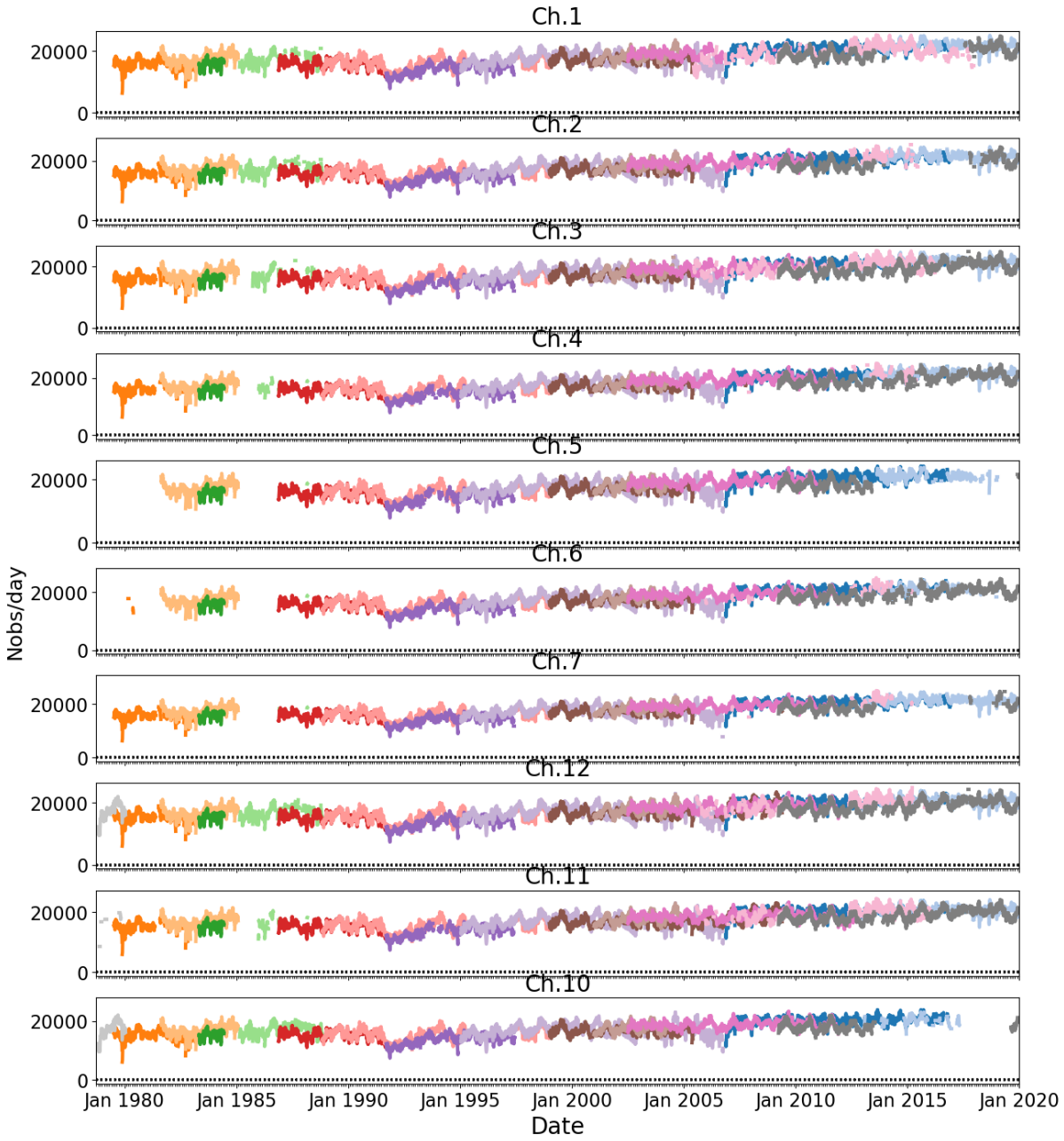

Figure 26: *Time series of the number of data per day used in the statistics.*

Figure 27 shows the mean difference between the observations and the simulations (bias). Except for channel 1, the variability of a single sensor is relatively small, because simulations remove important differences between the satellites (such as different orbital drifts, causing differences in diurnal cycle sampling, but also different spectral response functions). However, by using smaller y-range of 5K, compared to the results presented in section 4.1, differences between most sensors can be visualized. Only channels 6 and 11 show very small inter-satellite differences.

For channel 10, NOAA-12 shows a trend from low negative to almost neutral bias. This is related to SO_2 emitted by the Mount Pinatubo eruption in the first half of 1991. SO_2 has an absorption line at the edge of the spectral response function of channel 10 of NOAA-12

(1223 cm^{-1}; RD 13). For NOAA-11, this is not found, because NOAA-11 channel 10 observes different wavelengths (795 cm^{-1}).

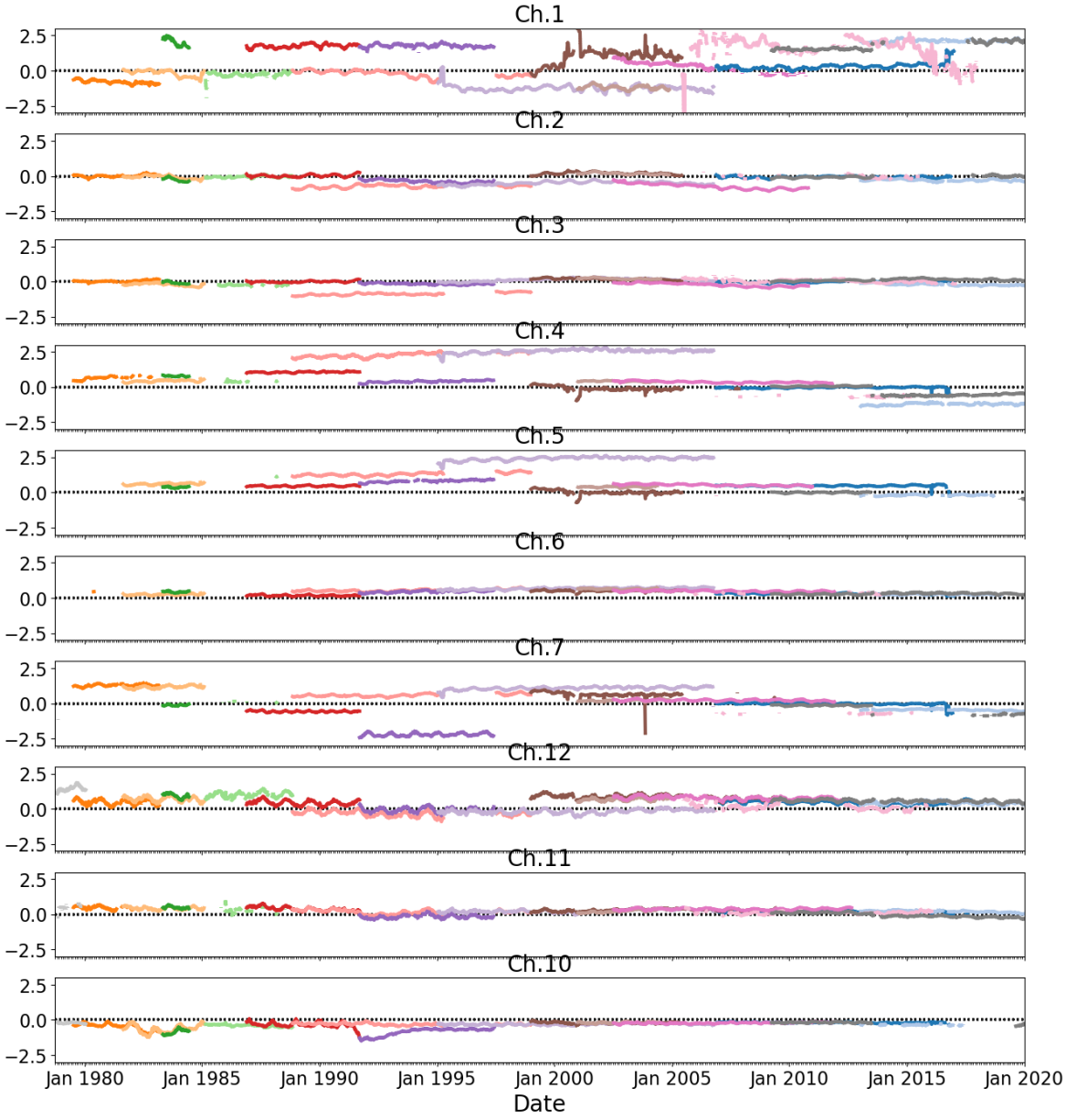

Figure 27: *Time series of the monthly bias with the standard error.*

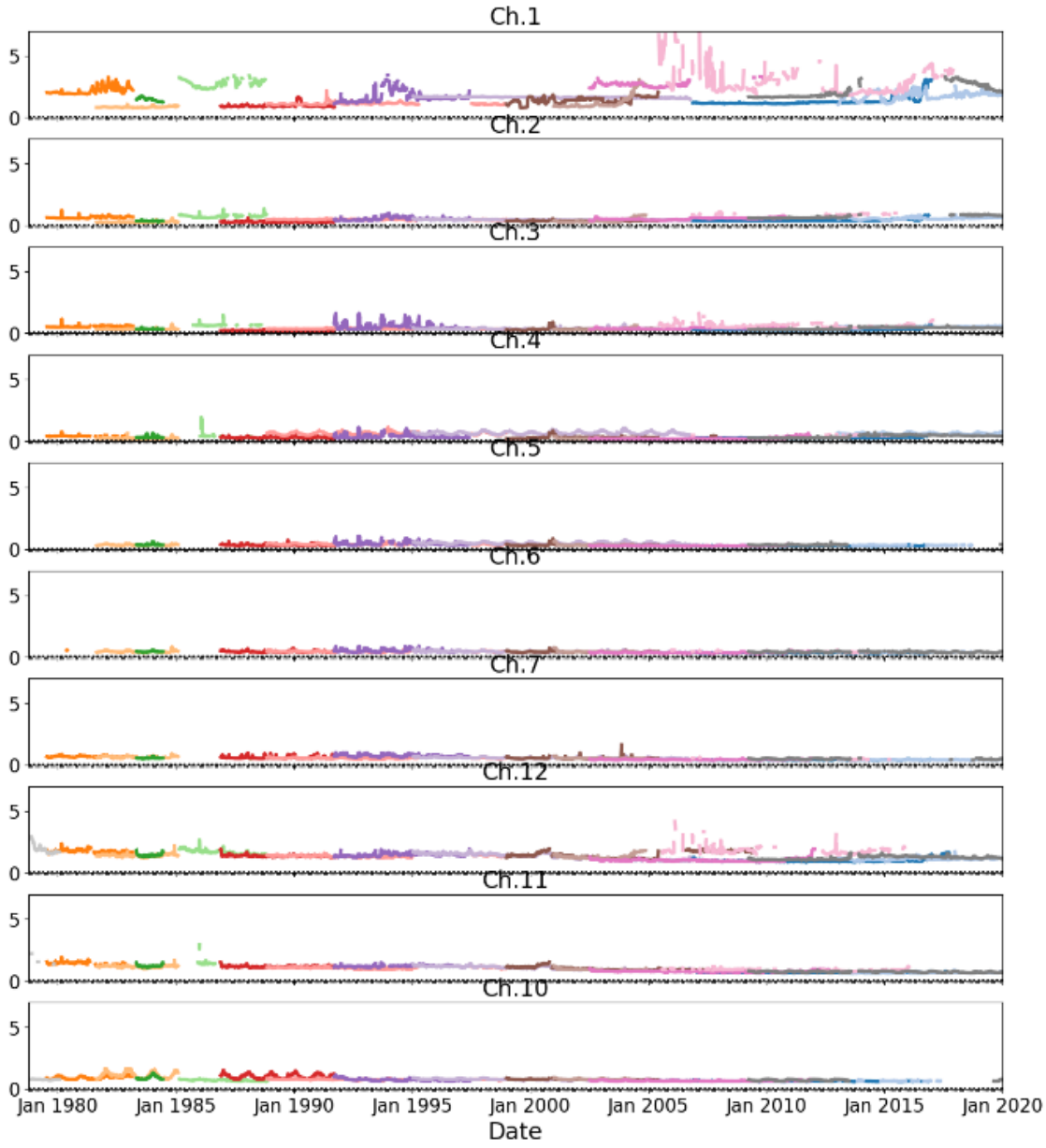

Figure 28: Time series of standard deviation of the bias shown in Figure 27.

Figure 28 shows the standard deviation of the bias with respect to the simulations. Results indicates rather good agreements, under 1 K for most channels, and generally steady over time. For water vapour sounding channels (10 to 12), one observes a small decrease over time (except for some satellites). Overall, this may be attributed to the improvement over time in the quality of the representation of the water cycle in ERA5 especially after the mid-1990s as reported by Hersbach et al. (2020, see section 9.2 “Global balance”).

To illustrate how the NEDT in the HIRS FDR (available for every pixel, every channel) can be used as a quality indicator, we point to Figure 29, to be compared with Figure 28. This shows that the removal of noisy episodes by QC1 clearly yields more stable time series. Noisy episodes can be seen in time series of the warm NEDT in Figure 30. The removal of these episodes by QC1 is shown in Figure 31.

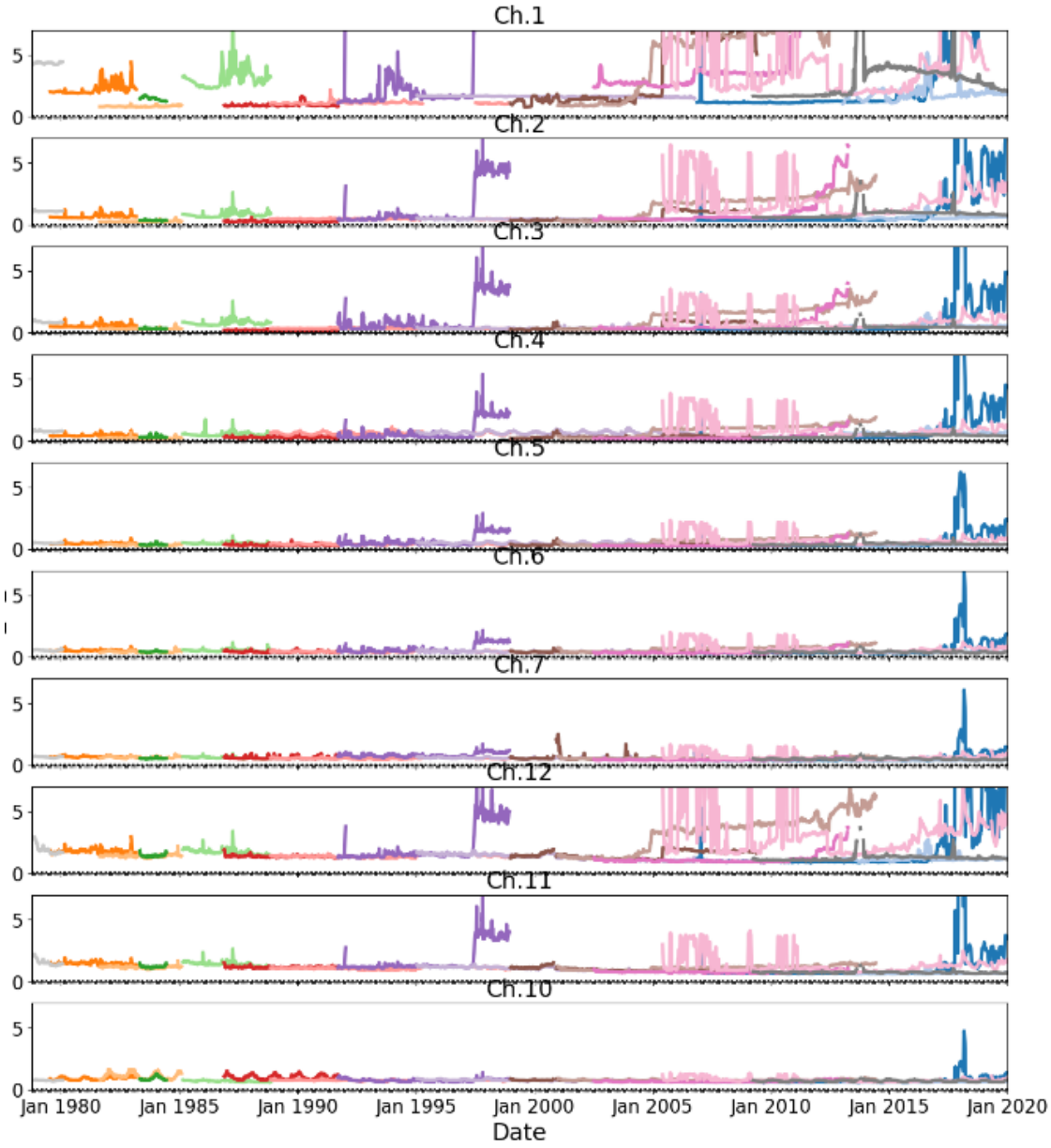

Figure 29: *Similar to the previous figure, but without applying QC1 (i.e., no removal of noisy episodes).*

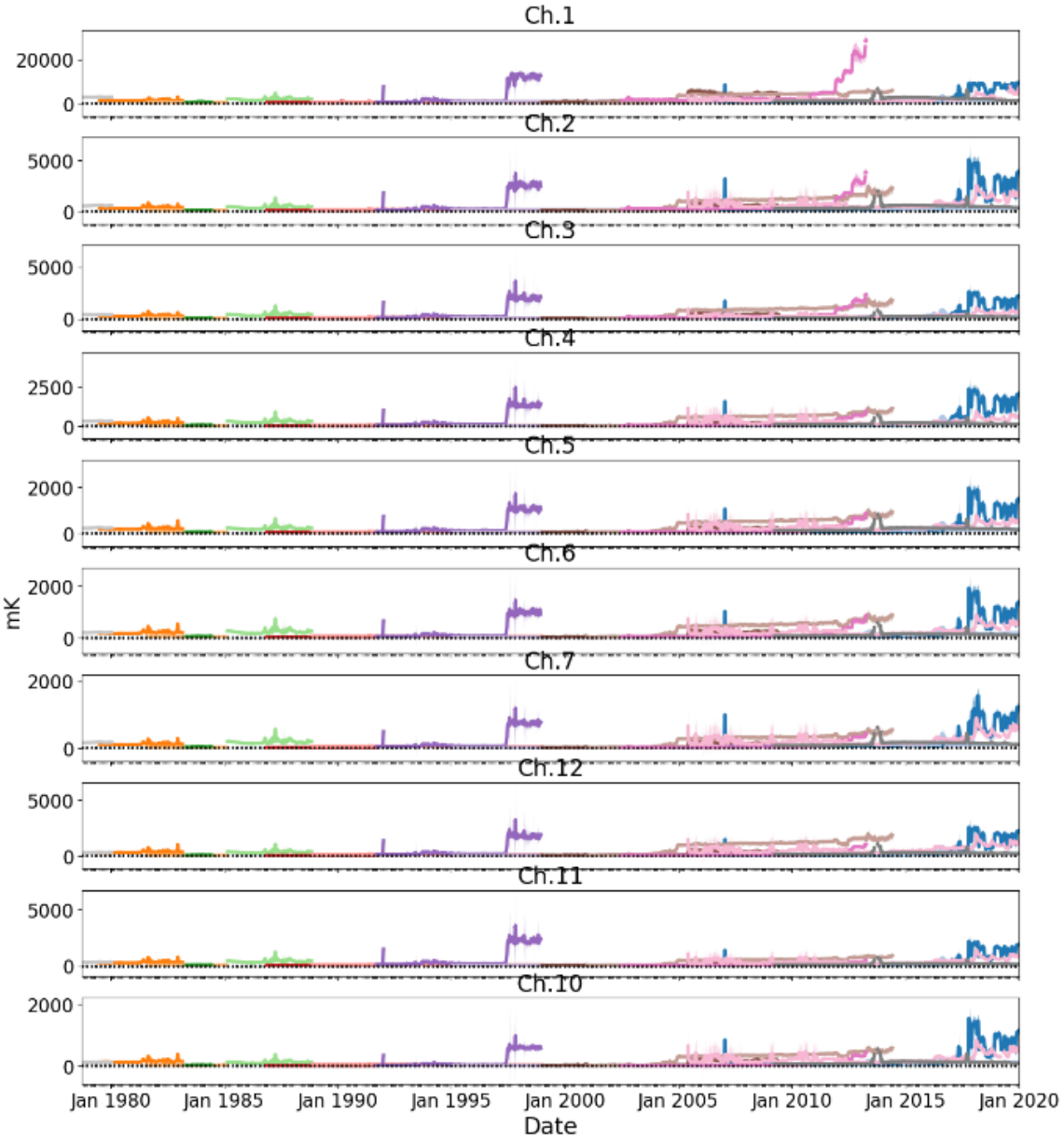

Figure 30: *Time series of the mean NEDT for the warm calibration without applying QC1.*

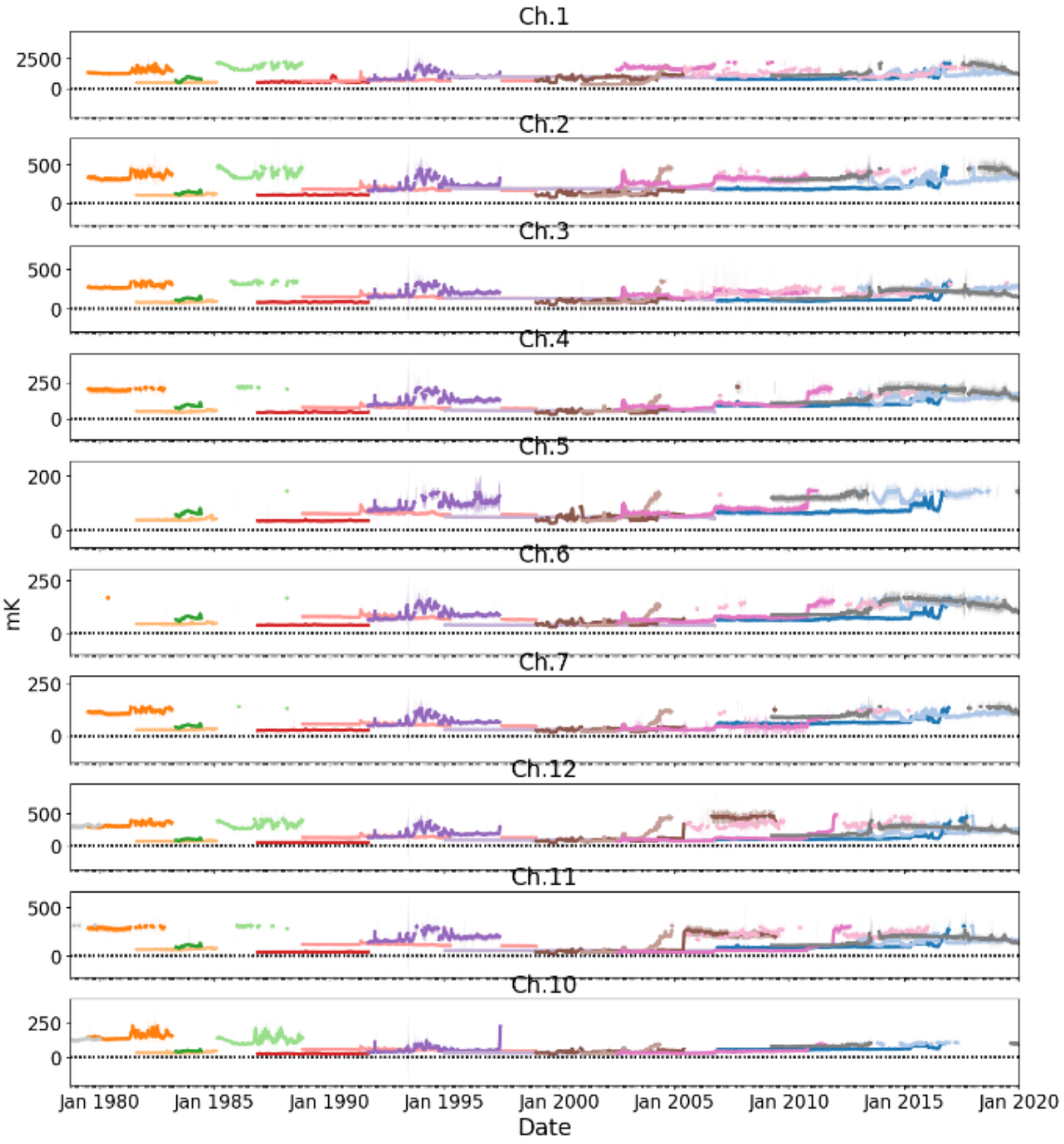

Figure 31: *Similar to the previous figure, but after applying QC1 (i.e., removal of noisy episodes). Note the drastic change in vertical scales.*

4.2.2 Surface sensitive and shortwave channels

We now discuss time series of the HIRS FDR observations compared to the simulated observations for the shortwave temperature sounding (channel 13 to 17), the surface sensitive (channel 18, and 19), and the ozone (channel 9) channels. The shortwave channels are sorted by the peaking weighting function from the upper troposphere (channel 17) to the lower troposphere (channel 13) or surface (channels 18, 19).

Figure 32 shows the number of observations after quality control and cloud screening. The shortwave channels show about half of the observations found for the other channels. These channels measure between 3.7 µm and 4.5 µm, where solar radiation reflected by the atmosphere contributes to the observations. These solar radiation contributions are difficult to

simulate and, thus, only observations with solar zenith angle larger than 100 degrees are considered below (QC3 in section 3.2.2).

This night-time selection causes a varying number of observations in the time series, because the satellite orbits are drifting over time. NOAA-15 for example is drifting from an early morning orbit through the twilight to a late afternoon orbit. NOAA-16 and NOAA-18 are as well drifting strongly. Channel 9 shows however the same stability as the other longwave channels, with the effect of Pinatubo eruption.

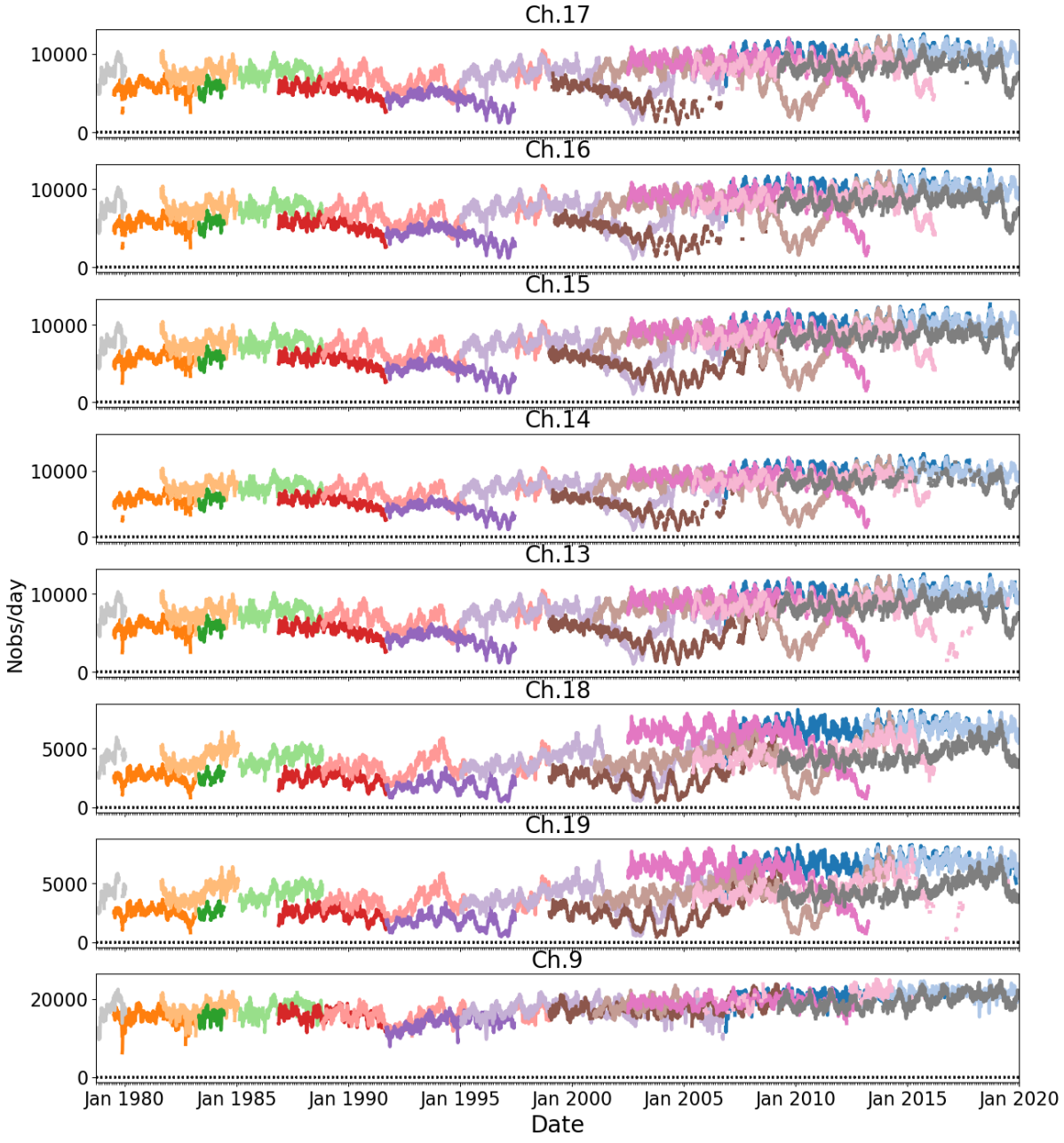

Figure 32: Time series of the number of data per day used in the statistics.

Figure 33 shows very stable time series of the bias for all sensors in the channels 18 and 19. Several instruments exhibit signatures of a changing annual cycle, which could be related to the drifting orbits, as the amount of night-time observations changed. The large inter-satellite

differences are not fully understood at this point, but could be related to night-time data selection (QC3). Such a masking results in selecting only some regions of the world, which vary over time and by satellite. This could expose regional biases in the reanalysis used for the simulations. Such biases would indeed remain hidden in the previous section, where the statistics were global. However, one does not observe here any coherence between the various satellites and channels located in the 4.3 µm CO_2 absorption band, as the shortwave channels are ordered here from highest-peaking (Ch. 17) to surface-sensitive (Ch. 18, 19). Another possibility for the differences could then rest with small offsets between the SRF of each instrument/channel and the SRFs assumed by RTTOV. Indeed, the absorption by CO_2 is much stronger at 4.3 µm than at 15 µm, giving rise to sharper weighting functions (e.g., Susskind and Kouvaris, 2006), and then conversely to an increased sensitivity to the SRF accuracy.

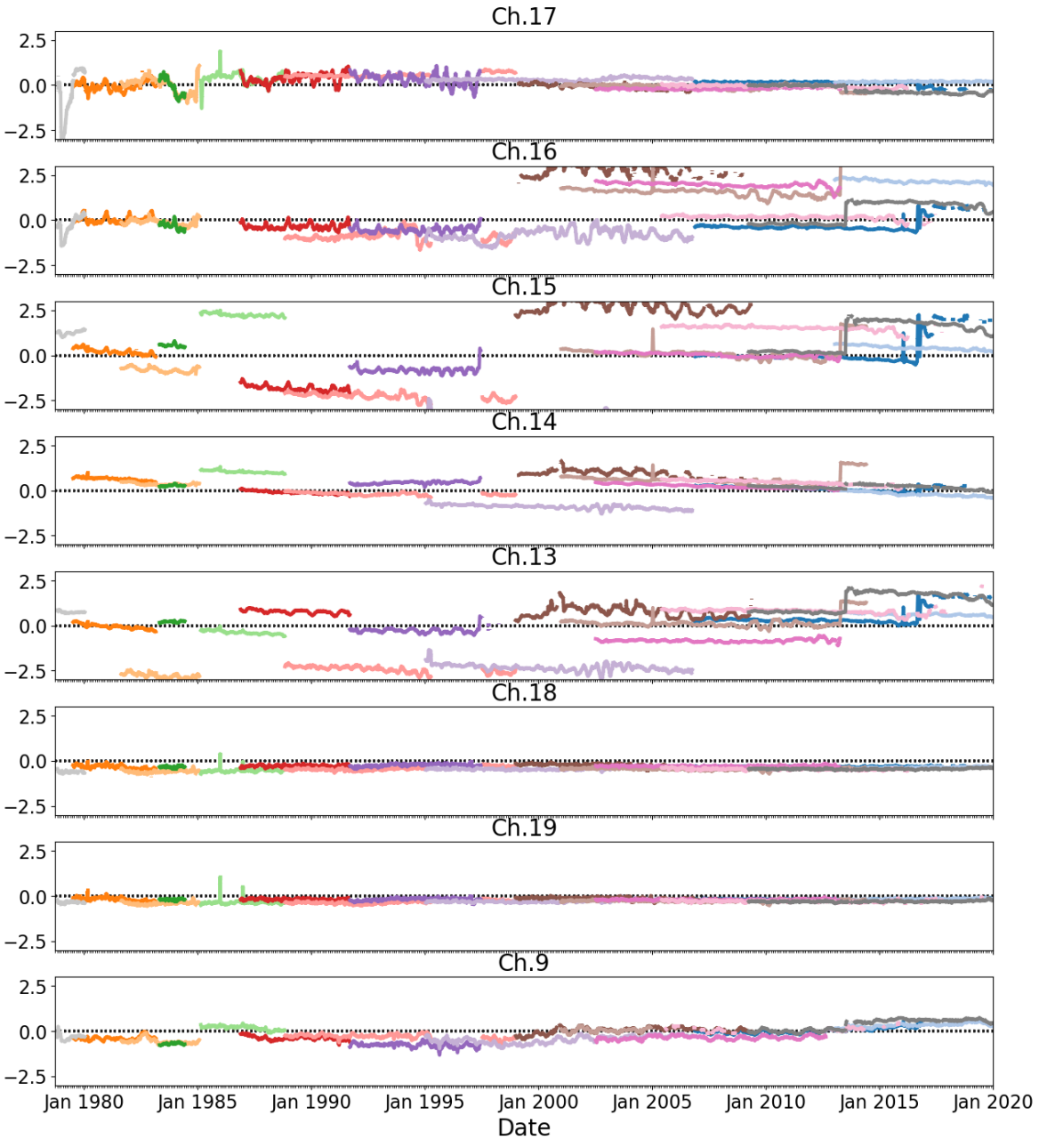

Figure 33: Time series of the monthly bias with the standard error.

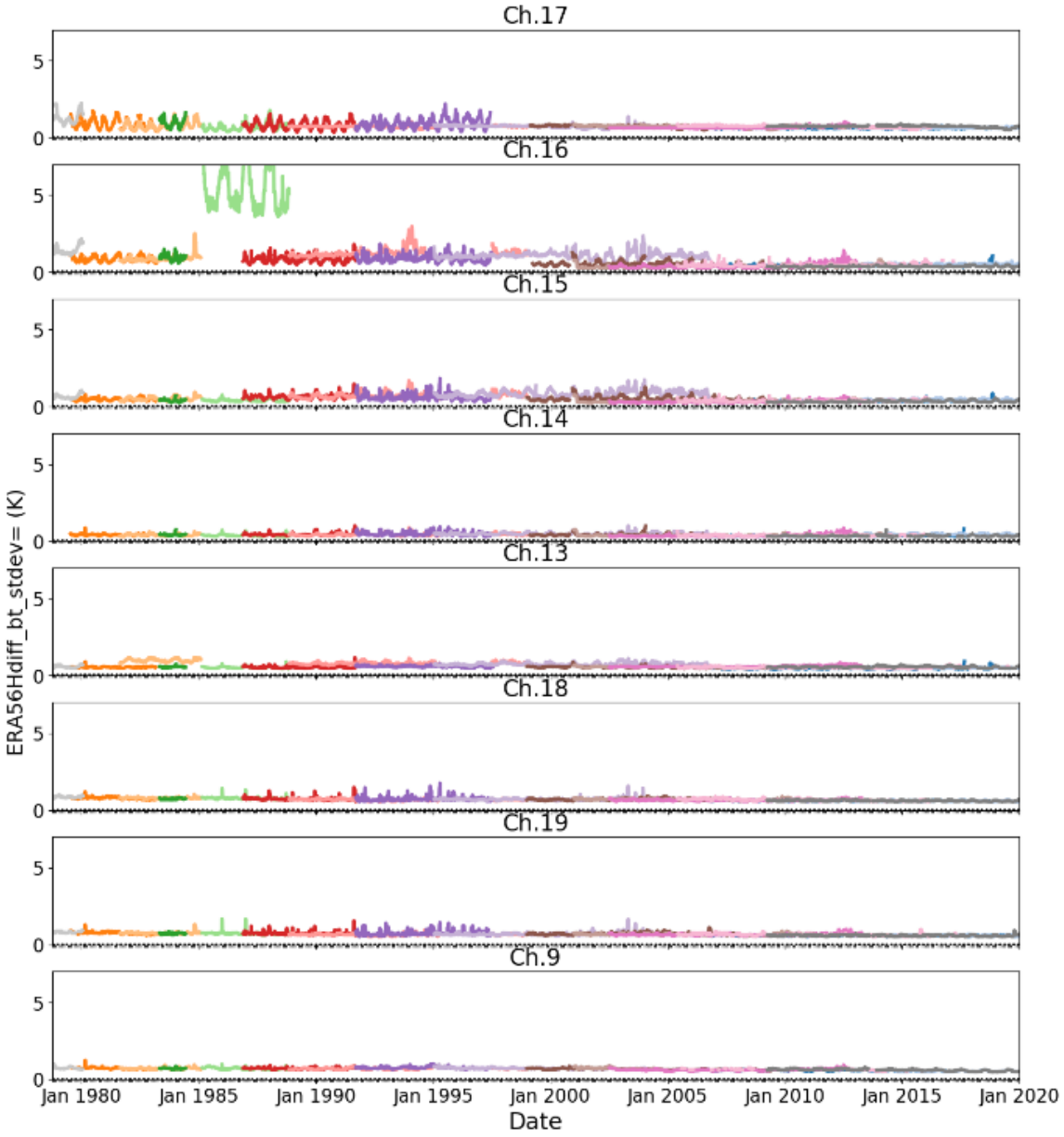

Figure 34: *Time series of standard deviation of the bias shown in Figure 33.*

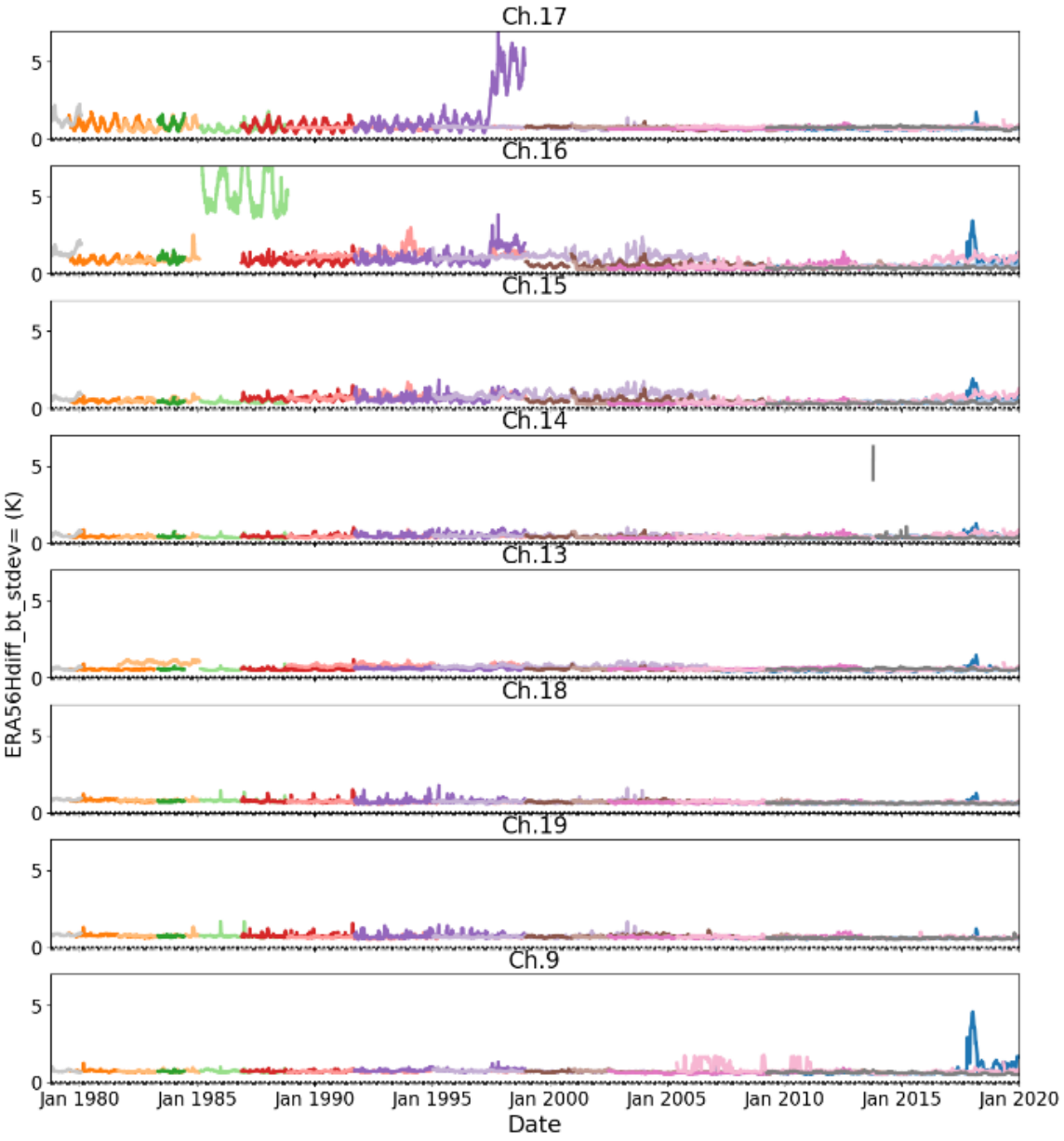

Figure 35: *Similar to the previous figure, but without applying QC1 (i.e., no removal of noisy episodes).*

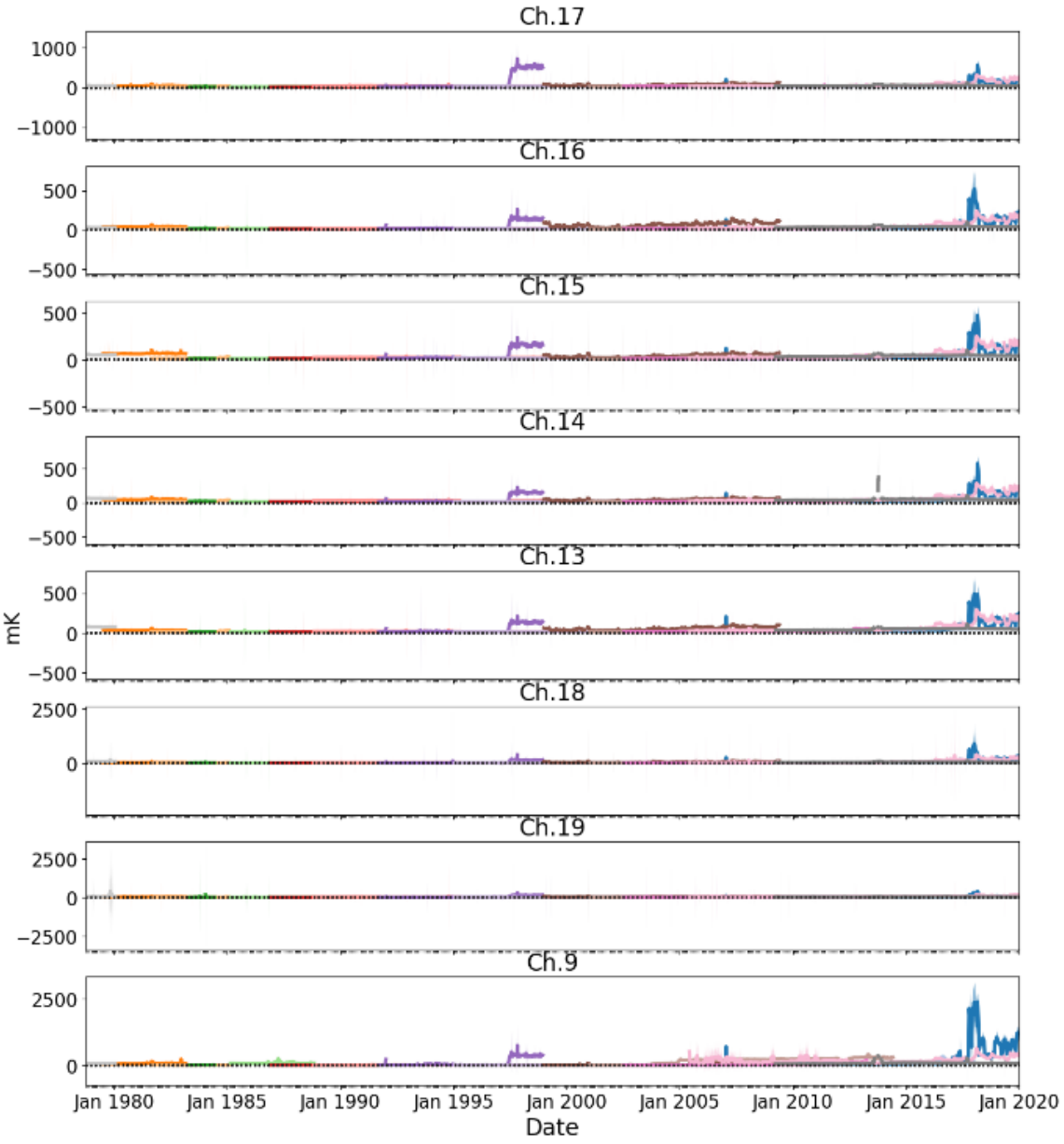

Figure 36: *Time series of the mean NEDT for the warm calibration without applying QC1.*

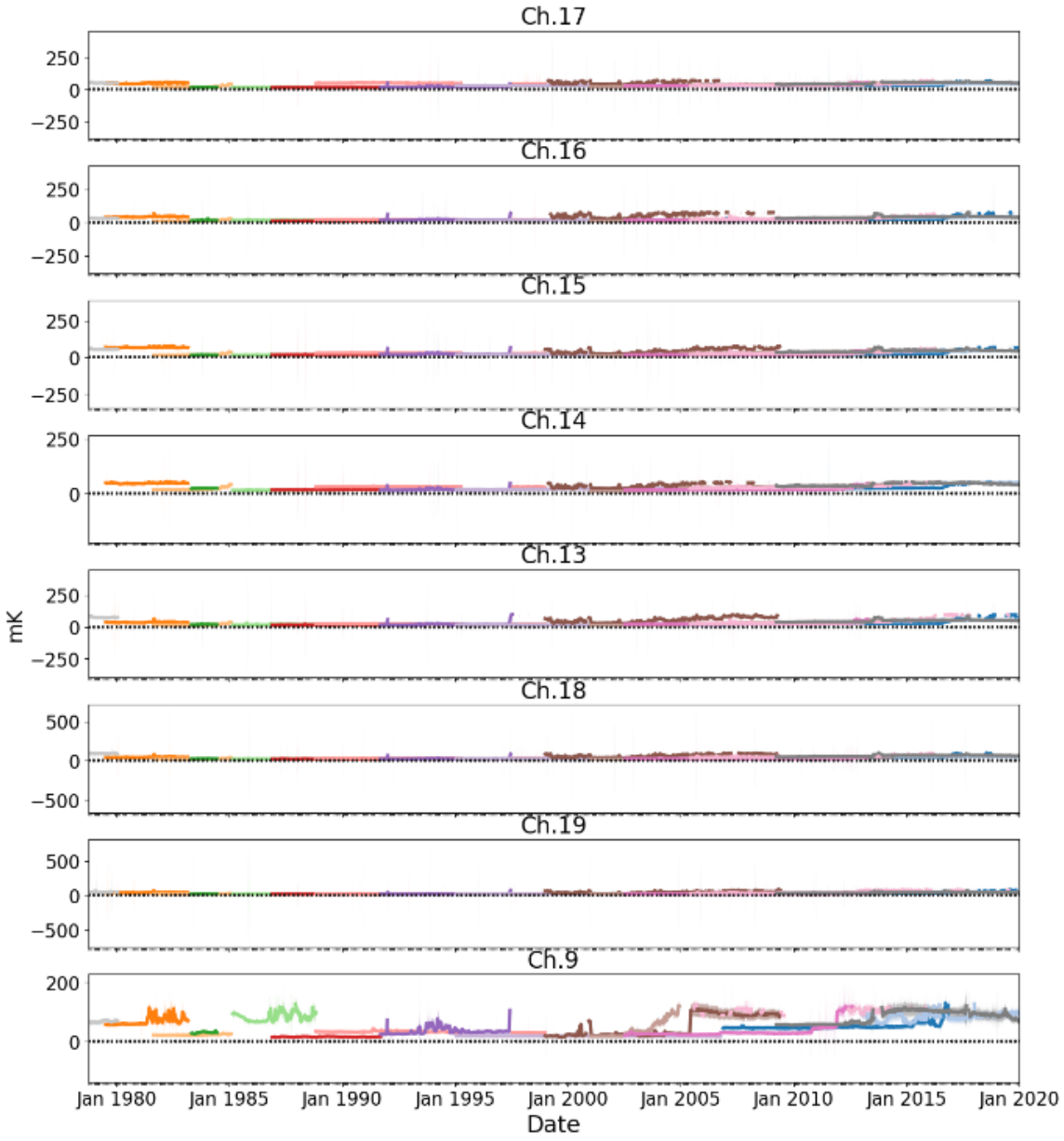

Figure 37: *Similar to the previous figure, but after applying QC1 (i.e., removal of noisy episodes). Note the drastic change in vertical scales.*

The standard deviations of the bias shown in Figure 34 and Figure 35 show the impact of applying QC1, to filter out noisy episodes visible in Figure 36 (and largely removed in Figure 37).

In summary, the results in section 4.2 show similar results compared to the time series analysis in section 4.1. The main remaining issues of the HIRS FDR for direct climate applications are related to inter-satellite biases. The individual sensors show a stable behaviour beside the issues already mentioned with NOAA-12, NOAA-18, NOAA-19, and Metop-A.

Further, these results demonstrate the usefulness of the NEDT, for example to support a further quality filter to the data.

4.3 Improvements against operational calibrated data

This section shows the impact of the two following major improvements in the HIRS FDR Release 1, as compared to the operational data: quality information:

- the noise equivalent differential temperature (NEDT) is computed and provided for every scanline and channel for all HIRS instruments, as a measure of the instrument noise;
- the data quality indicators are available in the FDR Release 1 for all HIRS instrument models.

Quality information was previously not always available, or not calculated consistently, for the different HIRS instrument models. This makes it difficult to compare the quality information in HIRS FDR Release 1 with the operational processing, because it did not include all the quality information that is generated by AAPP V4. For this reason, we revert to comparing selected metrics of the FDR that do not exploit any quality information with metrics that do.

The metric that is chosen here is the standard deviation of the brightness temperatures over a day. This reflects the natural variability, as each HIRS sensor covers the Earth twice a day, as well as the instrument noise and other uncertainties (e.g. changes in calibration). The data sample considered is the same as described in section 3.2.2. The results are shown in panels (a) and (c) of Figure 38, noting here that QC1 is not applied. Considering individual time series, large deviations from the mean values are sometimes visible, for example for channel 12 on NOAA-12, NOAA-18, and Metop-A, channel-14 on NOAA-19, channels 18 and 19 on NOAA-12, or spikes for channels 6, 7, and 10 on NOAA-15. In contrast, panels (b) and (d) in the same figure show that applying QC1 removes many noisy episodes well.

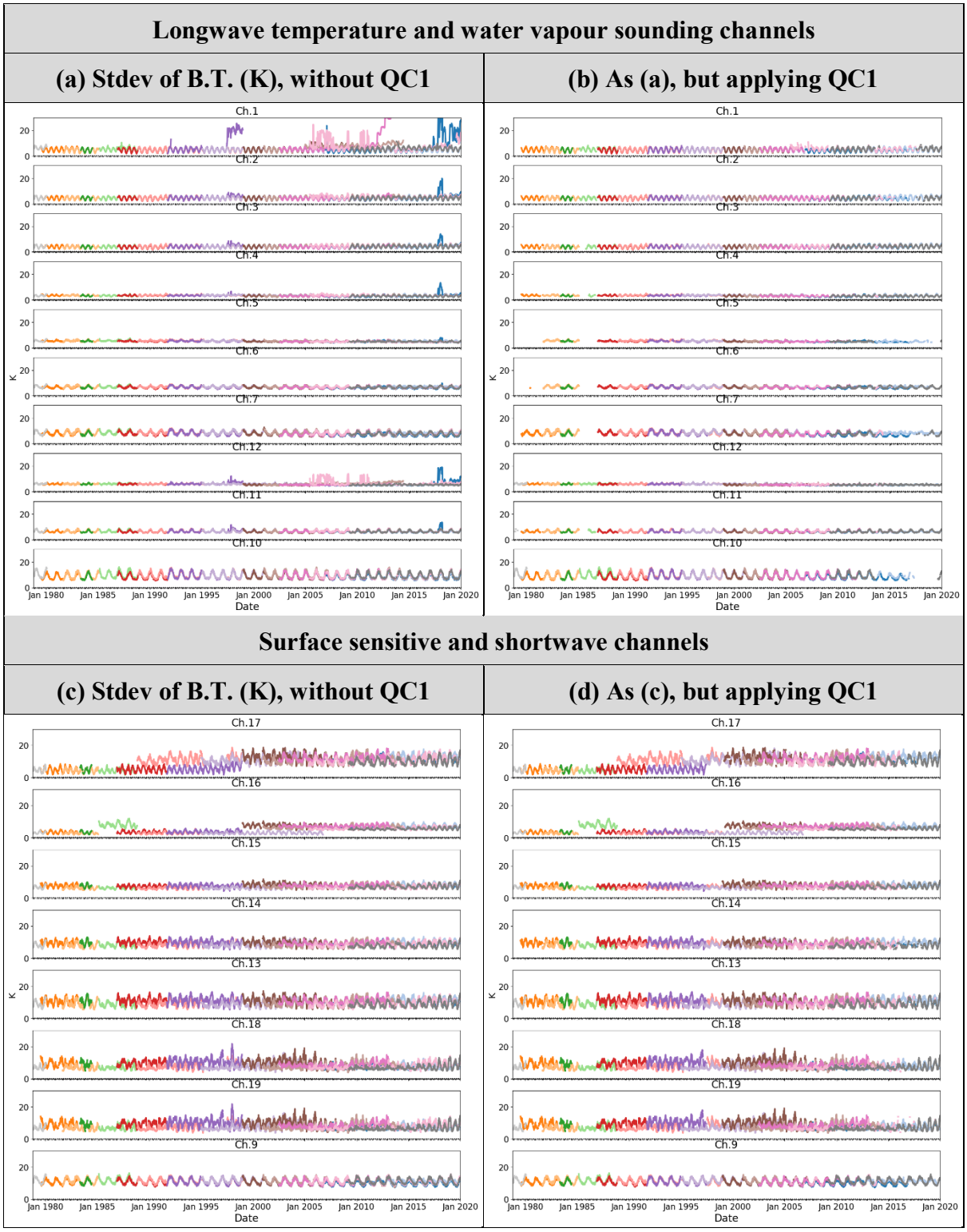

Figure 38: Time series of standard deviation of the FDR daily standard deviation in brightness temperatures without (left) or with (right) removal of noisy episodes (QC1). See Figure 25 for the legend.

5 SUMMARY AND CONCLUSIONS

This report presents the validation results of the first release of the HIRS level 1 Fundamental Data Record generated through a full recalibration and reprocessing of all HIRS data available at the NOAA CLASS archive.

This release includes four major improvements compared to the operational data, which have been validated above:

- More than one calibration cycle is used to compute the calibration slope and offset, which reduces strong variations in the calibration coefficients between two or within a super swath;
- The instrument self-emission is considered and a model for computing its impact is implemented;
- The noise equivalent differential temperature (NEDT), as a measure of the instrument noise, is computed and provided for every scanline and channel for all HIRS instruments;
- The data quality control has been updated and applied throughout the FDR identically.

The results presented above, show a clear improvement of the HIRS FDR compared to the original data. This can be expressed by (1) higher stability of the calibration on the short time range especially within a super swath; (2) the consistent usage of the NEDT over the entire data set to remove noisy data. Both factors together make this recalibrated data record more consistent and more accurate compared to the original data. However, not all issues with the HIRS data record could be resolved and especially the inter satellite biases still remain.

A combination of not considering the instrument status and a revised outlier removal of the calibration measurement provide more brightness temperatures in the HIRS FDR, especially for NOAA-15, -18, and -19. The uniformly processed NEDT allows the user, in those cases to decide on the use of certain pixel measurements, instead of discarding possible valuable data due to binary quality flagging. In particular, the mentioned missing NEDT (section 3.1.1) in the original data for some years is now filled with valid NEDT data and the due to the usage of the NEDT as quality threshold provides access to more data. Two examples of threshold for rejecting data based on NEDT specifications were shown in this report (1.0x and 1.25x specifications), but users are free to select other settings depending on their application.

Generally, some periods have been identified to show reduced quality especially in the longwave channels. This is mostly related to problems with the filter wheel. These periods are:

- NOAA-12 after summer 1997;
- Metop-A after 2015;
- NOAA-18 most of its lifetime;
- NOAA-19 after July 2013;
- NOAA-16 after 2004;
- NOAA-9 especially after fall 1986.

These periods show an increased NEDT, where daily mean NEDT is out of specifications (see Table 3). However, the user can use the updated NEDT to filter out all pixels, which NEDT is actually above a certain threshold.

The comparison to the simulated temperatures show generally low biases, except for channel 1. The biases for single instruments is found to be very stable in time but between the

instruments, larger biases were observed. The shortwave channels show for some instruments changes in the annual cycle, which is most likely related to the orbital drift. In addition, the NEDT provides a good measure to detect periods with larger standard deviation in the biases, which further supports the usage of the NEDT as an additional filter for high quality observations, mentioned above.

6 REFERENCES

Number	*Document Name*
RD 1.	Algorithm Theoretical Baseline Document - HIRS FDR Release 1,EUM/OPS/DOC/20/1204897
RD 2.	Product User Guide – HIRS FDR Release 1, EUM/OPS/DOC/20/1182511
RD 3.	GCOS-154, 2011: Systematic Observation Requirements for Satellite-Based Products for Climate, 2011 Update, December 2011, 139 pp.
RD 4.	NOAA POD GUIDE – 11/98 Revision, NOAA
RD 5.	NOAA KLM users's guide, NOAA NESDIS, 1999
RD 6.	Atkinson, N., 2020: AAPP User Guide, NWPSAF-MO-UD-036. https://nwp-saf.eumetsat.int/site/download/documentation/aapp/NWPSAF-MO-UD-036_Userguide.pdf
RD 7.	Hocking, J., R. Saunders, A. Geer, and J. Vidot, 2019: RTTOV v13 Users Guide. NWPSAF-MO-UD-046, v1.0.2, 29/10/2020. https://nwp-saf.eumetsat.int/site/download/documentation/rtm/docs_rttov13/users_guide_rttov13_v1.0.pdf
RD 8.	Hocking, J., 2021: Radiance Simulator v3.0. User Guide. NWPSAF-MO-UD-051 v0.5 26/04/2021. https://nwp-saf.eumetsat.int/site/download/documentation/rad_sim/user_documentation/RadSim_UserGuide.pdf
RD 9.	Hersbach, H., and Co-authors, 2020: The ERA5 global reanalysis. *Q. J. Roy. Meteorol Soc.* **146**: 1999– 2049. doi:10.1002/qj.3803.
RD 10.	Krzeminski, B., N. Bormann, G. Kelly, T. McNally, and P. Bauer, 2009: Revision of the HIRS cloud detection at ECMWF. EUMETSAT/ECMWF Fellowship Prog. Res. Rep. 19. https://www.ecmwf.int/sites/default/files/elibrary/2009/10561-revision-hirs-cloud-detection-ecmwf.pdf
RD 11.	Cao, C., Jarva, K., & Ciren, P. (2007). An Improved Algorithm for the Operational Calibration of the High-Resolution Infrared Radiation Sounder, *Journal of Atmospheric and Oceanic Technology*, *24*(2), 169-181
RD 12.	Borbas, E., Feltz, M., 2019: Updating the CAMEL surface emissivity atlas for RTTOV. NWPSAF-MO-VS-058
RD 13.	Guo, S., Bluth, G. J. S., Rose, W. I., Watson, I. M., and Prata, A. J. (2004), Re-evaluation of SO_2 release of the 15 June 1991 Pinatubo eruption using ultraviolet and infrared satellite sensors, *Geochem. Geophys. Geosyst.*, 5, Q04001, doi:10.1029/2003GC000654.
RD 14.	Leroy, S. (2001), The effects of orbital precession on remote climate monitoring, *J. Clim.,* **14** (22), 4330-4337. doi:10.1175/1520-0442(2001)014<4330:TEOOPO>2.0.CO;2.
RD 15.	Chung, E.-S., and Soden, B. J. (2010), Radiative signature of increasing atmospheric carbon dioxide in HIRS satellite observations, *Geophys. Res. Lett.*, 37, L07707, doi:10.1029/2010GL042698.
RD 16.	Shi, Lei. (2013). Intersatellite differences of HIRS longwave channels between NOAA-14 and NOAA-15 and between NOAA-17 and METOP-A. IEEE Transactions on Geoscience and Remote Sensing. 51. 1414-1424. doi:10.1109/TGRS.2012.2216886.
RD 17.	Susskind, J., and Kouvaris, L. (2006). Contribution of the AIRS shortwave sounding channels to retrieval accuracy. *Proc. SPIE 6233, Algorithms and Technologies for Multispectral, Hyperspectral, and Ultraspectral Imagery XII*, 62331A (4 May 2006). doi:10.1117/12.665061.
RD 18.	NESDIS 29 The Complementary Roles of Microwave and Infrared Instruments in Atmospheric Soundings. Larry McMillin, February 1987. (PB87 184917/AS)